Energy for Sustainable Development 88 (2025) 101790

Contents lists available at ScienceDirect

Energy for Sustainable Development

journal homepage: www.journals.elsevier.com/energy-for-sustainable-development

Applying soft-link and geospatial methods for optimal hybrid microgrids and electric network designs: A case study on rural Mozambique settings

Berino Francisco Silinto [a,b,*], Darlain Edeme [c], Silvia Corigliano [c], Aleksandar Dimovski [c], Marco Merlo [c], Christian Zuidema [a], André Faaij [d,e]

[a] Department of Planning, Faculty of Spatial Sciences, University of Groningen, Landleven 1. 9747 AD Groningen, the Netherlands
[b] Department of Mechanical Engineering, Faculty of Engineering, University Eduardo Mondlane, Av. de Moçambique km 1.5, Maputo, Mozambique
[c] Polytechnic University of Milan, Piazza Leonardo da Vinci 32, Milan, Italy
[d] Integrated Research on Energy, Environment, and Society, University of Groningen, Nijenborgh 6, 9700 AE Groningen, the Netherlands
[e] TNO Energy & Material Transition, Utrecht, the Netherlands.

ARTICLE INFO

Keywords:
Optimisation
Grid routing
Hybrid renewable energy systems
GISEle
Geospatial planning
Rural electrification strategy

ABSTRACT

Decentralised-based hybrid renewable energy systems represent one of the cost-effective solutions for supporting access to and the provision of reliable and secure electricity services in rural developing regions. Electrification planning tools considering the specificities of targeted areas concerning uncertainties about energy demands and resources, including the technology-cost trends, are essential for proper system integration. This work, therefore, proposes a comprehensive geospatial-based optimisation modelling framework based on GISEle tool, which was expanded to size hydropower technology in addition to its integrated wind and solar capabilities. Moreover, its procedures were interlinked with two external open-source assessment tools: the SWAT model for hydro resource potential and RAMP for energy demand, combined with tailored publicly available geospatial and interview-based data. The newly expanded framework was applied to the Majaua-AP case study in Mozambique by modelling three evolving demand scenarios under two community-grid spatial scales to plan a cost-effective electrification strategy. The analysis results emphasise that communities with differing population sizes, and power pick values can be identified in any region depending on the project settings. Additionally, it revealed that local circumstances influence the best techno-economic sizing regarding optimal network distribution and hybrid microgrid configuration designs. The grid routing layout shows a good approximation compared to ground realities. For each community, a portfolio of generation system configurations including either diesel+renewables (PV/Hydro/diesel/batteries, PV/diesel/batteries) or 100 % renewables share (PV/hydro/batteries, PV/batteries, and hydro/batteries) were achieved. The latter becomes mostly attractive under fixed demand and high fuel price scenarios; among individual community-based system configurations, the net present costs (NPC) range from US$k41–5384 (grid expansion) and US$k152–22,562 (generation) while US$k19,156 (grid expansion) and US$k46,426 (generation) considering the whole region. The levelised costs of electricity (LCOE) ranged from US $/kW 0.112–0.247. Finally, the evolving demand including hydro in the technology mix allowed substantial LCOE reduction in most of the installed communities.

Introduction

The share of people with access to electricity globally is steadily increasing (IEA et al., 2020). Nevertheless, many people remain without access, disproportionally concentrated in rural areas of Sub-Saharan Africa (IEA et al., 2023). In these areas electrification is hampered by

Abbreviation: GISEle, GIS for Electrification; SWAT, Soil and water assessment tool; RAMP, Remote-areas multi-energy systems load Profiles; PV, Photovoltaic; NPC, Net present costs; LCOE, Levelized cost of electricity; RE, Renewable energy; DG, Diesel generators; BESS, Battery energy storage system; HRES, Hybrid renewable energy system; GIS, Geographical information system; GrdPts, Grid of points; Pf, Penalty factor; MinPts, Minimum number of points/people; Ɛ-Eps, Epsilon (radius of each single cluster); MV, Medium voltage; LV, Low voltage; PT, Power transformers; MILP, Mixed Integer Linear Programming; NG, National grid; SCN, Scenario; WT, Wind turbine; HT, Hydro turbine.

* Corresponding author at: Department of Planning, Faculty of Spatial Sciences, University of Groningen, Landleven 1, 9747 AD Groningen, the Netherlands.
E-mail address: b.f.silinto@rug.nl (B.F. Silinto).

https://doi.org/10.1016/j.esd.2025.101790
Received 11 October 2024; Received in revised form 28 June 2025; Accepted 7 July 2025
Available online 24 July 2025

poor infrastructure and services and limited capacity to generate income, making grid extension rather uneconomical (Lucas, Dagnachew, & Hof, 2017). Decentralised/off-grid renewable energy (RE)-based hybrid microgrids (Bhattacharyya, 2012) represent an increasingly viable and cost-effective alternative (IEA et al., 2020). Hybrid renewable energy systems (HRES) integrate one or more locally available RE generation sources, often combined with backup diesel generators (DG) and/or battery energy storage systems (BESS), interconnected to a local distribution network delivering electricity to consumers. HRES can offer continuous 24/7 reliable and potentially secure electricity supply services (ADB, 2017; Come Zebra, van der Windt, Nhumaio, & Faaij, 2021; Lian, Zhang, Ma, Yang, & Chaima, 2019).

Sizing HRES infrastructure requires adjusting designs to area-specific conditions (Peters, Sievert, & Toman, 2019). Geographical and climatic conditions influence resource availability and related technologies. Socioeconomic conditions and communities' spatial distribution, including energy demand and existing (road/electric) infrastructure also influence design solutions. Electrification may subsequently create changes in (latent) demand, which may give rise to further challenges to socioeconomic drivers (Riva, Ahlborg, Hartvigsson, Pachauri, & Colombo, 2018), which are critical factors to consider (Pfenninger, Hawkes, & Keirstead, 2014). Similarly, technology learning curves and related cost trend figures (Elia, Kamidelivand, Rogan, Gallachóir, & B., 2021) are also crucial to consider (Elia, Kamidelivand, Rogan, Gallachóir, & B., 2021; IRENA, 2024). Given these challenges, project failures are prone to occur (Ikejemba, Schuur, Van Hillegersberg, & Mpuan, 2017; Zebra, van der Windt, Olubayo, Nhumaio, & Faaij, 2023) which often follow inadequate planning and management due to neglecting local realities (Ikejemba, Mpuan, Schuur, & Van Hillegersberg, 2017).

Energy planning and modelling tools support the proper design of HRES. Previous studies on this field (Urban, Benders, & Moll, 2007; van Beeck, van Groenendaal, van Helden, & Ouwens, 2000) signal that developed tools should explicitly incorporate the conditions of developing countries. Furthermore, such tools ideally can respond to uncertainties following both spatiotemporal dimensions while being open-source and relying on open-data (Pfenninger et al., 2018; Pfenninger, DeCarolis, Hirth, Quoilin, & Staffell, 2017). Consequently, there is a call for combined and integrated frameworks that consider geospatial data and analysis. Specifically, those relying on sequential modelling steps reflecting the different electrification planning phases, i.e., combining territory analysis (population settlements, demand, resource assessments, etc.) with identifying least-cost solutions on generation capacity and network designs as interlinked blocks of analysis (Moner-Girona et al., 2018).

Several tools and methodologies exist for analysing HRES designs for rural electrification. Some present relatively limited modelling capabilities, while many rely on closed-source software and explicit working licenses that impede customisations for implementing new features, as opposed to those relying on open-source tools (Pfenninger et al., 2017). These considerations led to a review study by (Silinto et al., 2025) of possible GIS-based and HRES models for rural developing country applications. After reviewing 27 models in detail, the limits of available tooling were confirmed. The following five, were identified as most promising for such purposes: HOMER® (Saiprasad, Kalam, & Zayegh, 2018), iHOGA (Dufo-López, Cristóbal-Monreal, & Yusta, 2016; Saiprasad et al., 2018), GeoSIM (IED, 2021), IntiGIS (Angel, Dominguez, Guerra, Arribas, & Pinedo, 2011; Arias, 2015), Network planner (Kemausuor, Adkins, Adu-Poku, Brew-Hammond, & Modi, 2014; NP, 2019), and OnSSET (ONSSET, 2021). Nevertheless, even these mentioned tools miss key features, including open-source, multiple RE technologies, and sophisticated network design capabilities (Silinto, Edeme, et al., 2025).

In addition to being closed source-based tools, HOMER and iHOGA, for instance, integrate single-node modelling approaches on a technology-type simplified and aggregated level. Consequently, both underplay spatial parameters by aggregating sparsely located energy system elements (loads, resources, electric grids, etc.) into single nodes (Prina, Manzolini, Moser, Nastasi, & Sparber, 2020), hence, limiting network and geospatial data considerations (Silinto, Edeme, et al., 2025). In contrast, GeoSIM, IntiGIS, and OnSSET apply GIS-based modelling approaches combining geospatial techniques and data to inform optimal electrification solutions and supporting policies (Korkovelos, Khavari, Sahlberg, Howells, & Arderne, 2019). GIS-based tools benefit from the increasing availability of global open-access spatial datasets (Falchetta, Pachauri, Parkinson, & Byers, 2019), which would be a standard methodology choice for implementation in scarce data locations of rural developing regions (Cader, Pelz, Radu, & Blechinger, 2018). Moreover, these existing tools are also capable of combining with the available ground data, helping get robust energy analysis and results (Falchetta, Pachauri, Byers, Danylo, & Parkinson, 2020). Additional comparison on the tools' capabilities is summarised in appendix Table G.1.

This study relies on the recently developed tool, GISEle_V01, to propose an alternative modelling framework to support rural electrification planning challenges. GISEle is a fully open-source GIS-based tool, written in Python and developed under the Energy for Growing initiative of the Department of Energy of Politecnico di Milano, Italy (Corigliano, Carnovali, Edeme, & Merlo, 2020). GISEle, accessible on GitHub (E4Growing., 2022), has a graphical user interface, facilitating its usability by non-user programmers. Its modelling capabilities rely on multi-node approaches by evaluating cost-effective network and supply technology options in a high-level spatial granularity, either for off-grid or on-grid electrification solutions in both small- and large-demand scales (Corigliano et al., 2020).

A recent study developed by the authors (Silinto, Edeme, et al., 2025) adjusted the GISEle_V01's original microgrid sizing structure to enable additional capabilities targeting this study's aims. This was achieved by first including evolving demand-based scenarios into GISEle analysis considering representative demand profiles created by RAMP, a bottom-up open-source and Python-based model (Stevanato et al., 2020). Secondly, GISEle's capacity for sizing hydropower technologies was enabled by adding a procedure on river flow rate and hydropower assessment linked to SWAT model (Arnold, Srinivasan, Muttiah, & Williams, 1998).

Therefore, this study applies and tests the improved procedures in a rural village, Majaua administrative post (AP) in Mozambique, aiming to assess and demonstrate the capabilities of the GISEle-based framework in performing techno-economic optimisation analyses for system hybridisation under the uncertain conditions of rural energy systems. To do so, this study firstly discusses acquiring and preparing appropriate data, using fieldwork and online data repositories. Secondly, it adds evaluations of technologies' related cost trends complemented by several demand-based scenario analyses to help compare alternatives on hybrid microgrid systems-based capacity expansions to plan a solid and cost-effective rural electrification strategy. These attempts represent a step-forward contribution and novelties to the previous studies (Corigliano et al., 2020; Vinicius, Silvia, Aleksandar, Massimo, & Marco, 2021).

This study is thus structured as follows: Section "Material and methods" describes the methodological steps taken in using the GISEle framework, while also explaining the changes made and the scenarios developed. Section "Results and discussions" presents the ressults and discussions of the modelled scenarios. The concluding remarks and steps forward are summarised in Section "Conclusion and next steps".

Material and methods

This section explains the five-stage methodological procedures (Fig. 1). The first stage involves the extension of the GISEle modelling tool (Section "Applying the improved GISEle-based framework"), The second stage is data collection and preparation, drawn from open-access

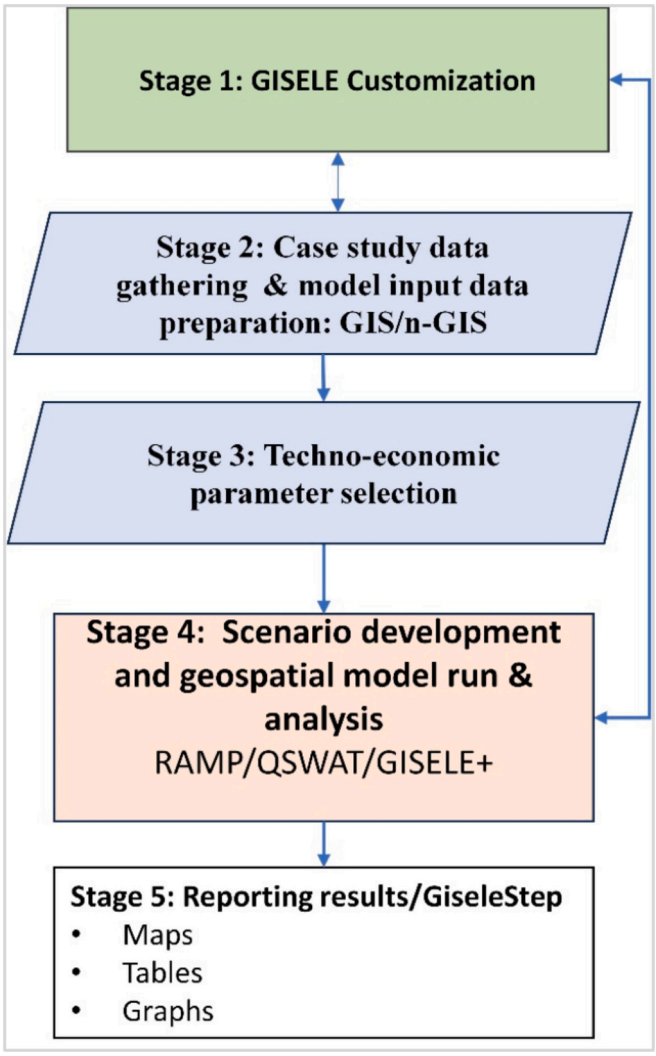

Fig. 1. Flowchart of the proposed five-stage methodological framework.

databases, reports, and field surveys (Section "Data collection and refinement (GIS data processing)"). The third stage assesses relevant techno-economic parameters including related cost data inputs required in GISEle (Section "Techno-economic and cost-data assumptions"). The fourth stage is developing and implementing different demand scenarios and foreseen technology cost assumptions along project timeframes (Section "Developed scenario description"), inspired by the uncertainties earlier highlighted regarding the changes in rural socioeconomic patterns and future developments after electrification. Stage five is the discussion of key results (Section "Results and discussions").

Applying the improved GISEle-based framework

The case analysis uses the upgraded GISEle_V0.1, whose original algorithms are explained in (Corigliano et al., 2020; Vinicius et al., 2021). The extensions with RAMP and SWAT uses are explained in detail in a separate MethodsX article (Silinto, Edeme, et al., 2025). This section only discusses the GISEle's central functionalities, including its application in the case of Majaua-AP. After data collection and preparation (Stage 2, Section "Data collection and refinement (GIS data processing)"), the framework (Fig. 2) relies on four integrated modelling steps, each focusing on specific rural electrification purposes and problem-solving.

The GIS data analysis (Step 0) starts by importing the case's grid of points (GrdPts) geospatial file (details in Section "Data collection and refinement (GIS data processing)") into GISEle and setting the working resolution (e.g. 200x200m/1000x1000m). The territory under analysis is spatially assigned in each centroid of its square pixel to the different features of its surrounding grid cells such as population density, elevation, slope, land use/cover, protected area, etc., used in the different procedures of the framework. The GrdPts is internally processed using a weighted strategy based on concepts proposed by (Etherington, 2016; Monteiro et al., 2005). The characteristics of terrain at each spatial point are translated into unitary (n) penalty factor (Pf) associated with a cost surface file (addressed in Appendix A) which, in terms of costs cumulatively (from 0-n), defines the weight representing the degree of difficulty in deploying electric lines across the terrain. Additional information on this matter is referenced in (Corigliano et al., 2020; Vinicius et al., 2021).

Step 1 involves population clustering and load demand assessment. While using population density data, the procedure firstly employs clustering techniques to group populated data points into clusters of densely populated areas, representing community settlements to be strategically electrified. GISEle uses a spatial clustering analysis procedure based on the Density-Based Spatial Clustering of Application with Noise (DBSCAN) algorithm (Corigliano, Carnovali, Edeme, & Merlo, 2020; Schubert, Sander, Ester, Kriegel, & Xu, 2017). The algorithm can automatically detect and create arbitrary non-convex-shaped clusters that spatially identify the exact extension of high-density populated points and outliers (noise element), being sparsely located households (not clustered).

The clustering procedure identifies community sizes fulfilling prechosen criteria according to a minimum number of people (MinPts) within a given radius (Ɛ-Eps) of each community/cluster. Both MinPts and Eps parameters' values can be selected through sensitivity analyses which provide a rough indication of the resulting: (a) number of clusters, (b) percentage of clustered people, (c) ratio number of people and the clustered area. Moreover, this facilitates selecting the preferred options based on the project goals. Any choice on these parameters' values might result in specific techno-economic implications as described in (Vinicius et al., 2021). After identifying the communities, energy needs and power peak values are estimated based on reference daily load profiles. However, GISEle's capability to generate load profiles is limited, therefore, loads are externally generated. For such purposes, several modelling approaches, including top-down, bottom-up models and system dynamics (Herraiz-Cañete, Ribó-Pérez, Bastida-Molina, & Gómez-Navarro, 2022; Lorenzoni et al., 2020; Riva, Tognollo, Gardumi, & Colombo, 2018) have been previously proposed. The bottom-up approach is preferred for non-electrified rural developing areas (Riva, Ahlborg, et al., 2018). Notably in that context, detailed load demand modelling considering possible future growth scenarios should be addressed.

GISEle is, therefore, complemented by the RAMP model (Lombardi, Balderrama, Quoilin, & Colombo, 2019). RAMP generates synthetic daily load demand profiles, modelled using bottom-up approaches starting from three distinct input parameters: (i) user class type, (ii) number of users, and (iii) owned appliances per user including their usage patterns assessed through interview-based information, literature, and expert assumptions. The specific user(s) of class type might be a group of households, public (offices, schools, hospitals, etc.) or productive (shops, processing industries, etc.) facilities. Each user is discretised by building type/income, number and nominal power of owned appliances, daily functioning times, and possible windows/cycle. These features are parameterized within RAMP (description in Table B.1, Appendix B), as required by the user to code and model the load profiles.

The baseload demand assessment addressed in this study relies on demographic and socio-economic information collected from the Mozambique National Census (INE, 2017), and assumptions about currently owned electric appliances, usage and functioning patterns derived from on-site surveys and extracts from the World Bank Multi-Tier Framework (Bhatia & Angelou, 2015). Three user demand

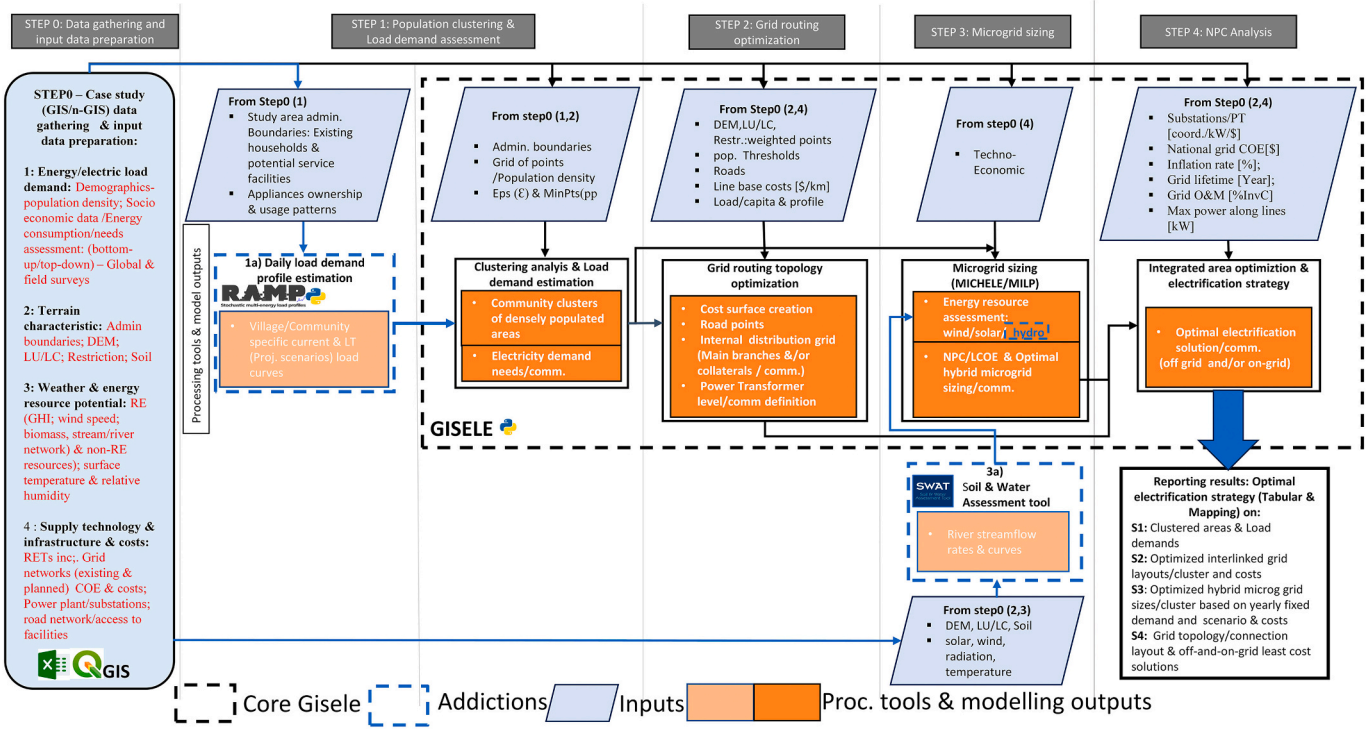

Fig. 2. Geospatial methodological framework based on the improved GISEle_V01 modelling procedures.
Note: It shows different procedures (coloured boxes), starting from GIS data collection and analysis: light blue; exogenous processing and input data generation tools: dashed blue (new developments to the previous release) (Corigliano et al., 2020); and core GISEle procedures and their modelling outputs: dashed black and orange.

classes/categories were identified; (i) households comprising three user levels: low (LIH), medium (MIH), and high (HIH) income, defined by type and quantity of owned appliances and monthly incomes; (ii) public/social facilities (10 users); and (iii) productive/commercial services (10 users), totalling 23 users. Features on the rated power, usage patterns, timing, and average total daily time uses of each owned appliance (described in Appendix, Table E.2) were also included. The generated load profiles are further input into GISEle while relying on a proxy number of households for each identified community and scaling up to the whole study area.

Step 2, the grid routing optimisation procedure is based on a geospatial topological approach that applies the Steiner tree concept (Corigliano et al., 2020). The imported GrdPts (Section "Data collection and refinement (GIS data processing)") and identified communities are the main inputs. The approach provides a reliable least-cost routing considering the hierarchical structure of a power system network composed of main branches and collateral lines (Vinicius et al., 2021). The analysis is based on GISEle's embedded graph theory algorithm explained by (Corigliano et al., 2020) and (Vinicius et al., 2021) where the procedure designs an optimal path of internal distribution grids connecting users/loads within each identified community. The grid routing algorithm firstly uses each community's aggregated load demand to internally derive their power peak levels based on the pre-computed reference load profiles and per capita values (Corigliano et al., 2020). Secondly, it designs the optimal internal grid layout to electrify each community. The routing follows road paths and is split in two electric line types; i.e., the main branch/backbone feeder and collaterals that connect the rest of the demand nodes. Furthermore, the algorithm computes the costs sustained for electrification, in terms of grid infrastructure required for either off-grid generation solutions (Step 3) and/or on-grid connections (Step 4). Nevertheless, based on their power peak levels, the requirements in terms of medium/low voltage (MV)/(LV) grid line types for allocating their corresponding power transformer (PT)/substation can be defined.

Step 3 involves the microgrid sizing procedure by applying a Mixed-Integer Linear Programming (MILP) model. The procedure identifies and generates the optimal hybrid microgrid generation portfolios able to satisfy the community loads in a defined timeframe, based on the available RE resources. The original GISEle algorithm only assesses wind and solar energy resources. This study applies the extended GISEle_V01 version enabled with hydropower sizing capabilities by using the SWAT+ model's river flow outputs. Linking GISEle to SWAT+ required improvements on its structure to import river flow discharges. Notably, these included GISEle customisations into the microgrid sizing algorithms to enabling hydropower technology. The Appendix C summarises the SWAT+ working procedures (Fig. C.2) including the linked features with GISEle. Table C.1 reports the key input data. Further details are addressed in Ref. (Silinto, Edeme, et al., 2025).

The upgraded procedure starts by assessing the available energy resources within the study area boundaries. The procedure downloads wind and solar energy resources internally from the website https://www.renewables.ninja/ an open-access database source developed by (Pfenninger & Staffell, 2016; Staffell & Pfenninger, 2016), and automatically computes their hourly/unit power profile time-series. The solar and wind yearly power profiles are further reshaped to consider a few typical days of the year to ease computation (Corigliano et al., 2020). The hydropower potential assessment and optimal sizing are constrained by the available river flow rate estimated by SWAT+, and the maximum radius distance to each associated community. These parameters influence the costs for direct grid connections. Finally, the procedure estimates the solar, wind, and hydro energy source potentials.

Subsequently, the microgrid sizing procedure combines the previously estimated load profiles with exploitable RE source potentials and the components' techno-economic specifications, and through simulations over the project timeframe, optimally sizes the hybrid microgrid generation solution including diesel generators (DG), solar photovoltaic (PV), wind turbines (WT), hydro turbine (HT) and/or BEES technology configurations that meet the peak load for each community-grid. Each

hybrid configuration is derived from an accurate modelling structure of integrated components and multi-year planning considering the asset degradation (Petrelli, Fioriti, Berizzi, & Poli, 2021). The NPC, Eq. (1), is the employed objective function to be minimised.

$$minNPC = \sum_i (IC_i + O\&M_i + RC_i - SV_i) \quad (1)$$

where: IC_i is the initial investment cost of components, $O\&M_i$ the yearly operation and maintenance costs, RC_i the replacement costs, and SV_i salvage (remained worth), each system component's value at the end of the system operation period. The generating technologies are represented by different sets, types, specifications, costs, and number of generators. The wider technology sets the higher computational efforts with a risk of non-convergence of the model. The details of the involved mathematical algorithms is fully addressed in (Petrelli et al., 2021).

Step 4, involves the NPC analysis (integrated area optimisation). The algorithm (formulated as a MILP model) supports an optimised techno-economic evaluation to define the overall electrification strategy for the study area chosen by comparing in economic terms a solution, either to directly connecting to an existing national grid (NG) substations/PT or through intra-connections among off-grid community-grids considering their voltage levels and network line distances as constraints. This process is completed by running the integrated Dijkstra algorithm (Corigliano et al., 2020; Vinicius et al., 2021) that finds the most feasible shortest-line path solution. To this end, both solutions are given per community settlement components compared through their NPC project costs and LCOE. The standard LCOE Eq. (2), is applied.

$$LCOE = \frac{\sum_{t=1}^{T} \frac{C_t + O\&M_t + F_t}{(1+r)^t}}{\sum_{t=1}^{T} \frac{E_t}{(1+r)^t}} \quad (2)$$

where C_t is the capital expenditure, O&M the operation and maintenance cost, F_t the fuel expenditure, E the electrical energy generated, t the year, and T the expected project lifetime. However, other specific LCOE formulations on the microgrid components and electrical equipment (MV/LV lines) costs including the utility wholesale cost of energy (COE) are applied (Corigliano et al., 2020) to finalise the selection of a cost-effective electrification strategy. To compare grid extension with off-grid electrification, the salvage value in Eq. 1, is considered for computing the NPC electric lines assuming a linear depreciation of each system component, considering 40 and 10 years lifetime for the electric grid lines and system respectively.

Data collection and refinement (GIS data processing)

Data collection for this study relied on a combination of extracting data from relevant research reports, datasets and fieldwork. The main sources were official reports and data repositories from the government (FUNAE,[1] EDM,[2] INE[3]), and other non-governmental, and international agencies (referenced in this study), dealing with or supporting the energy sector (Theo, Lim, Ho, Hashim, & Lee, 2017), complemented by collected data from interviews from August 2021 to April 2022. Most datasets were available and provided a comprehensive overview of Majaua-AP's energy profile, even though the spatial detail did not allow the identification of different clusters of energy needs. Socio-economic data, therefore, were complemented through site visits relying on surveys and interview-based questionnaires. Data on the existing population, resources, and techno-economic features were also insufficiently detailed to model the overall generation technologies. This gap was filled by using the global datasets in online open-access databases where geospatial and remote sensing energy-related data, such as population (Lloyd, 2017; Tatem, 2017), Digital Elevation Model (DEM): slope, land use/cover, weather (wind and solar), etc., derived from satellite imageries are stored.

Finally, the collected data needed processing into an appropriate-fitting geospatial format. The processing details are addressed in (Silinto, Edeme, et al., 2025)while datasets used in this study are listed in Table 1. This comprised both raster and vector layers clipped to the Majaua-AP boundaries. This allowed generating the study area grid of points layer resampled to 200 m working resolution.

Techno-economic and cost-data assumptions

The main technical-economic input parameters required to run the MILP procedure are reported in Tables D.1 and D.2 (Appendix D), including the full set described in Table D.3. Part of these inputs were derived from the literature (IEA, 2020; IRENA, 2022) and field data. However, most of the RE technologies' cost assumptions applied in the study scenarios (section 2.5) are extracted from (Allington et al., 2023; Cole & Frazier, 2023) that share several energy-related data for Mozambique in particular, on RE technology cost-trends until 2050 (Fig. D1, Appendix D). These trends are related to technology experience curves over the years. The latter represents the most prevalent method based on a log-linear equation relating the unit cost of a technology to its cumulative installed capacity or electricity generated. This method is commonly used to represent an endogenous technical change in large-scale energy-economic models that inform energy planning and policy analysis in which the characteristic parameter is the learning rate, defined as the fractional reduction in cost for each doubling of cumulative production or capacity (Elia et al., 2021; Glenk, Meier, & Reichelstein, 2021).

The hydro turbine details were chosen based on the river stream's average hydropower potential. A threshold limit was set to analyse rivers with potential for small scheme hydropower plants, that is, a capacity of <1000 kW (IEA-ETSAP & IRENA, 2015). The costs for deploying lines and assumptions on electrical parameters investments were derived from EDM (MIREME, 2018) and institutional website (https://www.edm.co.mz/en/website/page/electricity-tariffs).

Developed scenario description

This study relies on three demand evolution scenarios (SCN0–0 %, SCN1–2 % and SCN2–2.8 %), applied under two community-based spatial clustering and electrification expansion strategies (Section "Clustering communities and simulated load demand curves"): Strategy

Table 1
Input data used to generate the Majaua grid points and cost surface files.

Input parameter	Description	Source/website
Administrative boundaries	Vector layer-polygons	(GADM, 2022)
Population	Raster layer-100 m: population distribution	(CIESIN, 2020)
Infrastructure	Vector layer including facilities (health, school, water)	(INE, 2017)
Land use/cover project definitions	Raster layer-10/30 m: including10/22 land use/cover types	(ESRI, 2021)/JRC[a]
Elevation	Raster layer-30 m: NASA SRTM Digital elevation/slope	(Jarvis, Guevara, Reuter, & Nelson, 2008)
Protected areas	Vector-polygons	(UNEP-WCMC and IUCN, 2022)
Road network	Vector layer-lines/road networks	https://www.openstreetmap.org
Rivers	Vector: river flow rates from Global Runoff Data Centre	(GRDC (Global Runoff Data Centre), 2021)

[a] https://forobs.jrc.ec.europa.eu/products/glc2000/products.php

[1] National Energy Fund

[2] Electricidade de Moçambique (national grid utility)

[3] Instituto Nacional de Estatística (Mozambique Statistic Berau)

ClA starts with electrifying each of the identified cluster's groups of densely populated areas (communities). Strategy Cl0B electrifies the whole study area as a single community. The scenarios all assume the basic demand data on owned appliances and energy use per type of each demand class/category, i.e., household or service (public or commercial, etc.) as explained in Section "Data collection and refinement (GIS data processing)".

The developed scenarios differ in two ways: firstly, they assume different moments when household types or services adopt new electric equipment, expressed as a percentage and the year of adoption. Secondly, the scenarios differ in the expected energy demand growth next to the addition of such equipment, due to either population growth or intensified use of equipment. The study assumptions on the type and number of appliances owned by each user within each demand category are summarised in Table E.2, Appendix E. These values are the input parameters coded in RAMP to model the reference baseload profile applied in SCN0 which assumes a modest adoption of new equipment and no additional demand growth. Appendix Table E.3 (A&B) further details assumptions on the adopted appliances and the year of their appearance modelled in both SCN1 and SCN2 respectively. The middle scenario (SCN1) is slightly more ambitious regarding the adoption of equipment and assumes a 2.0 % additional annual growth of demand. The optimistic scenario (SCN2) has the most ambitious assumptions regarding the adoption of equipment and assumes a 2.8 % yearly growth of demand. The power per capita value required to estimate the pick power values for each identified community was defined by averaging the 15 different yearly reference load profiles.

The final NPC analysis step 4, defines the optimal electrification strategy. Georeferenced data on the existing substations linking the MV power lines were available and used as a reference input while assumptions on future connections were demonstrated. The consistency of all demand scenarios modelled runs under both ClA and Cl0B strategies over the project timeframe of 10 and 15 years, respectively. Additionally, the resource details and techno-economic and cost trends assumptions (Table D.1) were included in their corresponding scenario reference year. However, since the diesel cost is a variable parameter with highly fluctuating patterns, in addition to the model run reference diesel cost of 1 US$/l, a sensitivity analysis on costs was performed with two additional fuel cost ranges (Table D.2) to assess/understand how the microgrid size's techno-economic features is affected by the fuel cost variations. This information together with other technology-specific data (Table D.3) was loaded to determine the least-cost hybrid microgrid configurations, from which the electrification strategy and investment is advised. Fig. 3 illustrates the schematic workflow of the performed simulations.

Results and discussions

After presenting the case study area and its terrain analysis and the resulting cost surface map (Section "Case study area characterization"), this section further discusses the achieved simulation results. The clustering and demand assessment analysis (Section "Clustering communities and simulated load demand curves") identified community settlement and their energy needs. Sections "Internal grid routing design" and "Microgrid sizing: optimised electrification strategies-based scenarios" discuss the internal grid routing layout designs and optimised microgrid generation portfolios for each identified community-grids and the comparisons among demand scenarios. The sensitivity analysis is performed in Section "Sensitivity analyses on cost scenarios", with Section "NPC analyses/integrated area optimisation & electrification strategy" discussing the NPC analysis of the available electrification strategies.

Case study area characterization

Majaua-AP (Fig. 4) is a typical rural locality of Mozambique (48,777 inhabitants/139 inhabitants/km^2) (CIESIN, 2020). The area (418 km^2) has an irregular topography with terrain elevations between 350 and 1000 m above sea level. Majaua, comprises three main localities, namely Majaua-Maia, Dachudua (headquarters of Majaua-AP), and Zalimba located at 55, 39, and 24 km from the District of Milange headquarters, respectively. The locality relies heavily on agriculture and livestock and is served by unpaved roads in poor conditions (boulders, steeps, muddy in the rainy season, and slippery). Majaua is modestly electrified, with some localised cases of solar home systems and a 627 kW capacity mini-hydropower plant installed along the Ruo River (bordering Malawi and Mozambique). which is not operating since 2022 due to storm damage.

However, the geospatial data analysis generated a 200 m resolution grid of points file with terrain characteristics comprising 10,265 points (Fig. 5a). Water bodies are mostly concentrated in the west region, where the Ruo River flows. No protected areas were identified. The electrifiable population, amounting to 48,777 (CIESIN, 2020), are spatially distributed across the Majaua-AP village. Fig. 5b depicts the Pf values (explained in Section "Applying the improved GISEle-based framework"/Appendix A) at each pixel size of the terrain (coloured points), ranging from 1.5 (presence of roads) to 9.1 (along rock, steep and mud pavements, and forests).

Clustering communities and simulated load demand curves

Fig. 6 shows the output results of the clustering procedure for both the ClA (group of communities) and Cl0B (whole area) clustering solutions. In the first instance, 1000 and 328 and 1000 and 100 were the final Ɛ-eps and MinPts values selected for ClA and Cl0B solutions, respectively. Both were obtained by performing a sensitivity analysis, by varying *eps* (from 1000 to 3000 m) and *MinPts* (from 100 to 500 people) considering: (a) the resulting number of clusters, and (b) the percentage of clustered people in the area. The analysis maximised the number of people (>75 % in both solutions) to be electrified. By running the procedure with the aforementioned inputs, 13 communities were identified for ClA, with 70 % of the assessed area and 88 % of the total population of Majaua covered. The residual, 12 %, corresponds to the outliers (light blue dots); i.e., sparse individuals outside the clustered communities. Cl0B covered 48,769 (~100 %) people covering 99 % of the assessed area. In Appendix E further discussions on clustering and sensitivity analysis results are presented. The electrification analysis subsequently targeted either first electrifying each identified community (ClA) or immediately electrifying the whole study area (Cl0B).

Fig. 7 presents the generated reference daily load profiles aggregated for each demand category, using the RAMP model. The load profile for public service is explicitly shaped by public lighting services, which consequently influences the overall load curve. Independent of the size and their spatial location, household load curves featured an increase from 4 to 8 am then a decrease to midday peak demand, followed by a steady reduction until 5 pm. From 5 pm, a rapid increase in demand leads to a maximum peak consumption around 9 pm. Most households in Majaua AP are not yet connected to the grid, and therefore, a local grid expansion is simulated as a result of the evolving demand. The load profiles disaggregated by user type within each demand category are depicted in Fig. E.2 (Appendix E).

The estimated average load profiles were aggregated and scaled up for each community in both ClA and Cl0B scenarios according to their respective population and sizes. These profiles are essential for the determination of the demand peaks, a key input for sizing the microgrid generation capacities so that optimised generators and storage systems can meet each community-specific peak load. In this process, a minimum population threshold of 5 people per household and load per capita[4] value was the additional loaded parameters for computing the peak power values. Fig. 8 compares the estimated power peaks (Fig. 8.a)

[4] Amount of 0.0749 kW per person

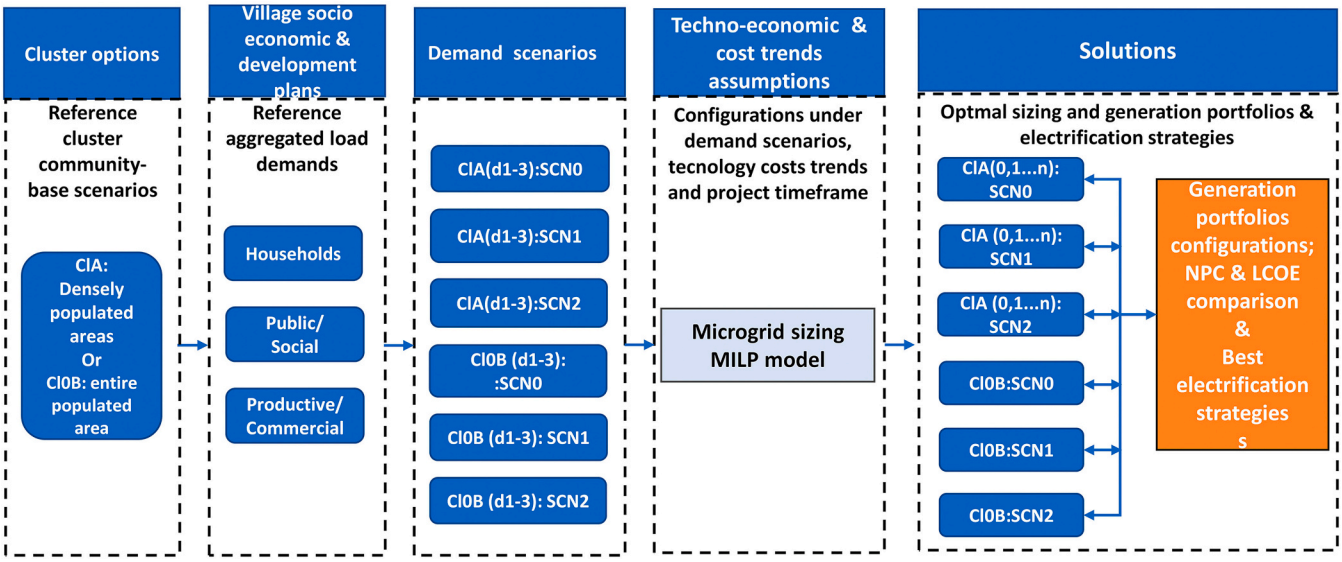

Fig. 3. Logic steps of the modelled scenarios.

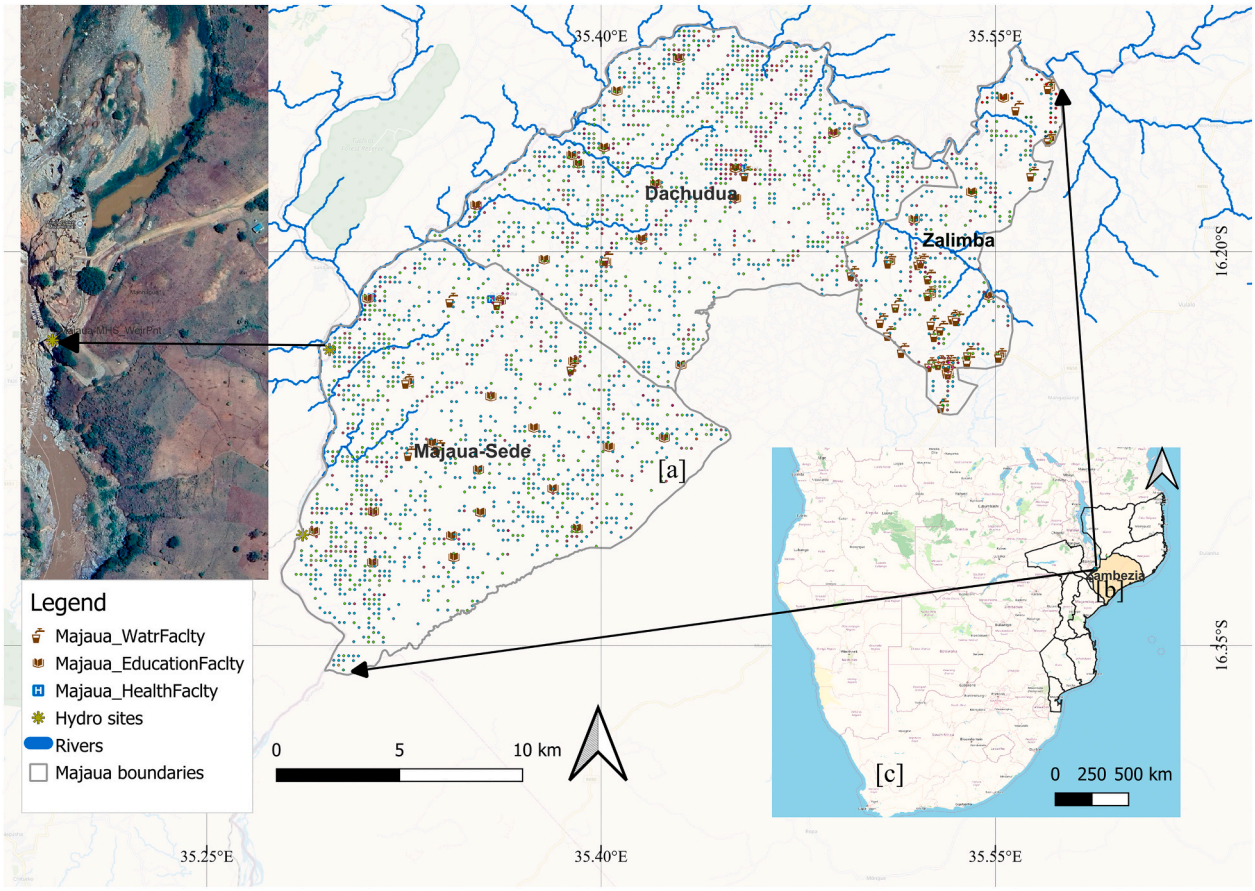

Fig. 4. Majaua-AP's geographical boundaries [a], Zambezia/Mozambique [b], Southern Africa [c], including the existing facilities.

together with estimated annual energy consumption (Fig. 8.b) targets among communities in the reference SCN0. The total sum of each community load to be served in ClA is 12 % lower compared to the Cl0B load (justified by residual people) which by serving them leads to an annual energy consumption of 183,835 (ClA) and 209,767 (Cl0B) MWh respectively.

With the reported peaks, planners can define the voltage level requirements for each community and define the suitable (MV/LV) feeders/PTs to be installed. For instance, communities owing load levels above certain thresholds such as e.g. >100 kW, communities 0, 2, 3, 5, 8, 9, and 12 (ClA), ranging from 104 to 1675 kW and Cl0B, 3653 kW, both should be connected through MV power lines either from off-grid generation sources or to the nearest available NG substation. In contrast, community loads <100 kW would be connected through LV power line-

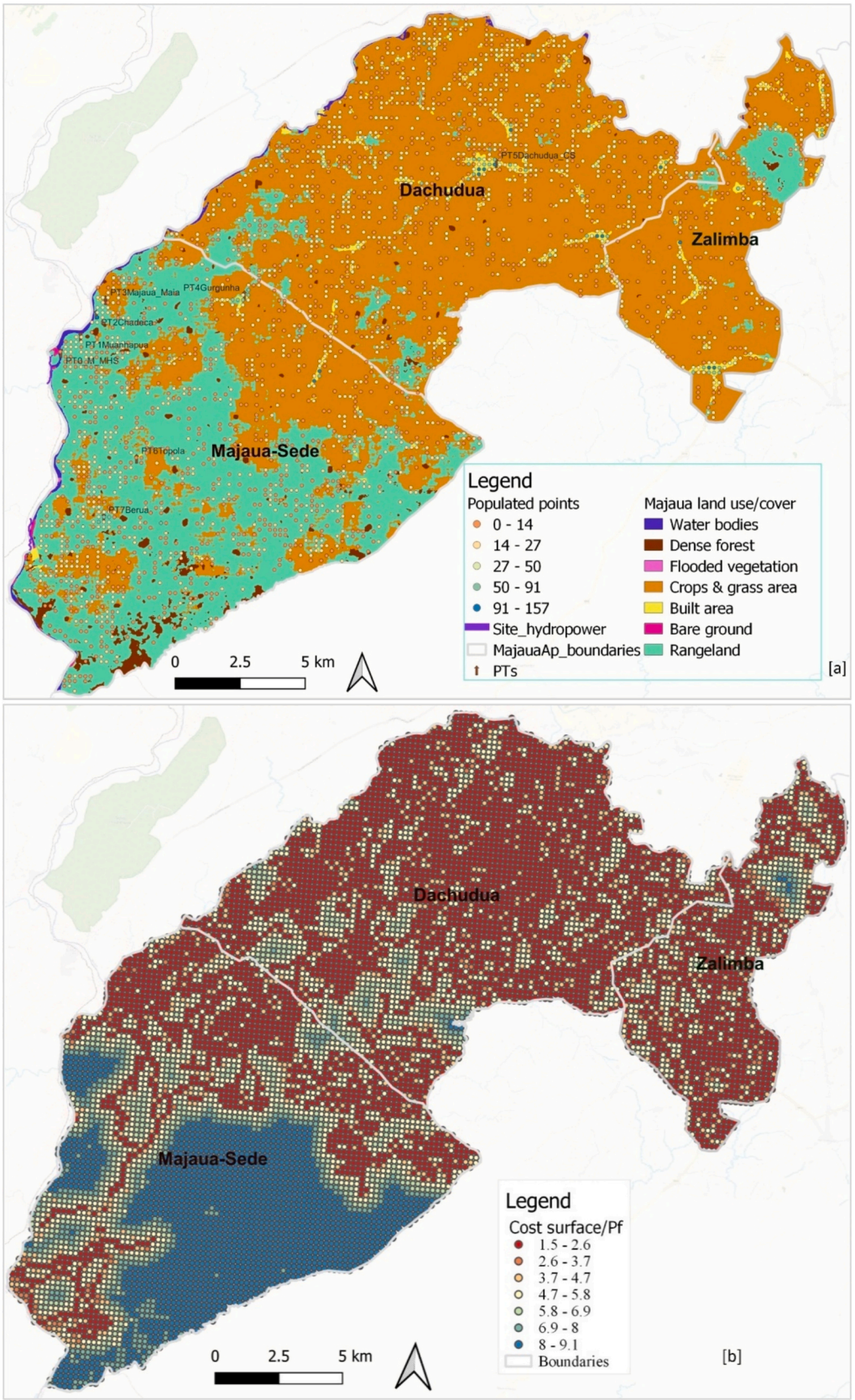

Fig. 5. a) Land use/cover map; b) Weighted grid of points (cost surface map) derived from terrain analysis.

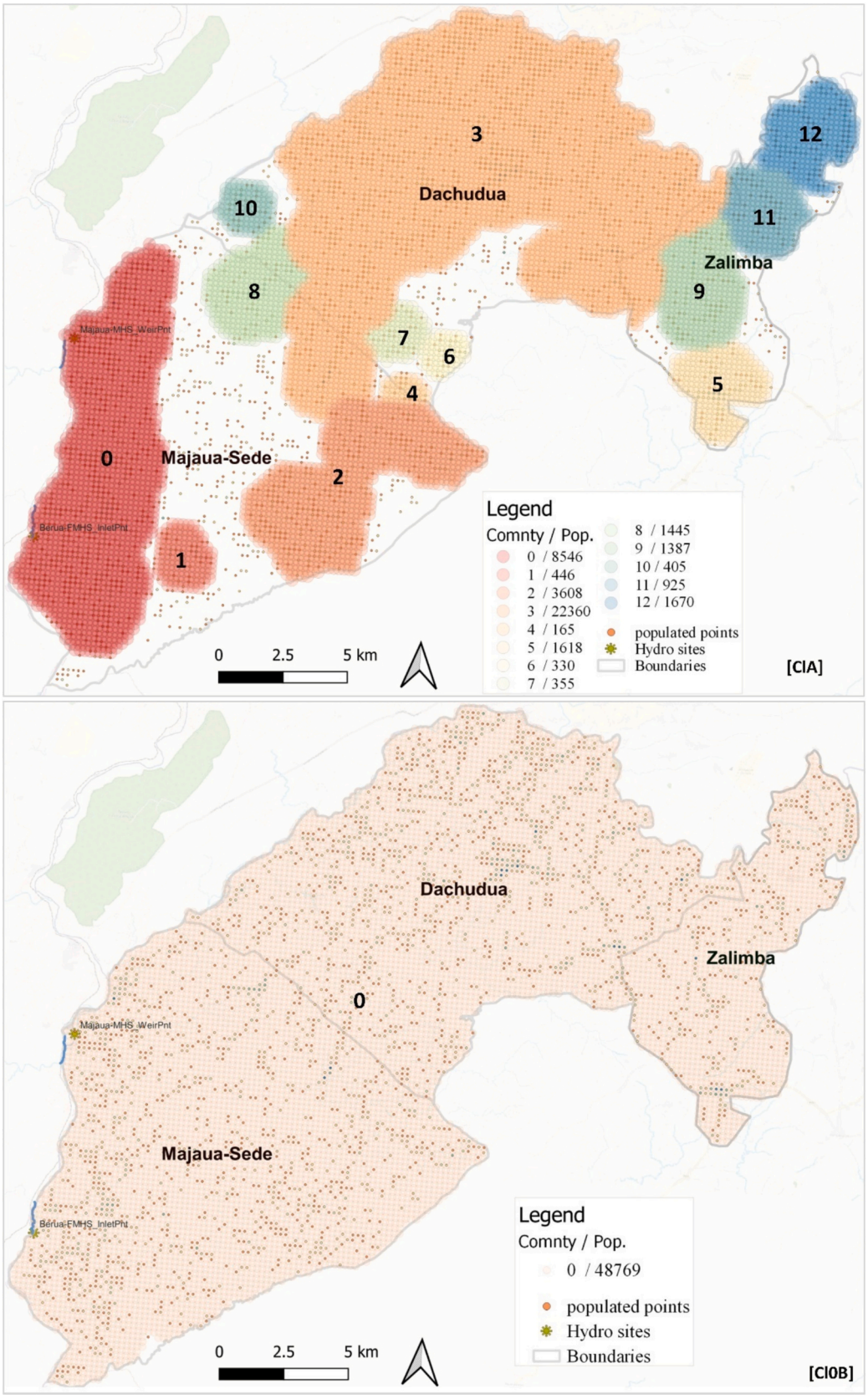

Fig. 6. Identified densely populated cluster/communities and population sizes in (ClA) and the representative single community (Cl0B) (entire administrative area) of Majaua AP to be electrified.

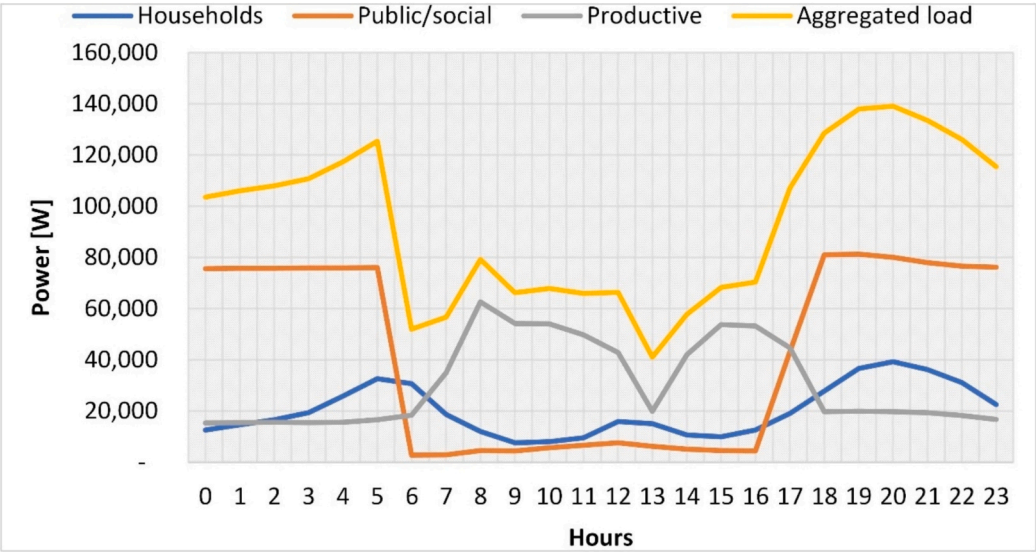

Fig. 7. Daily load profiles for representative user categories resulting from surveys.

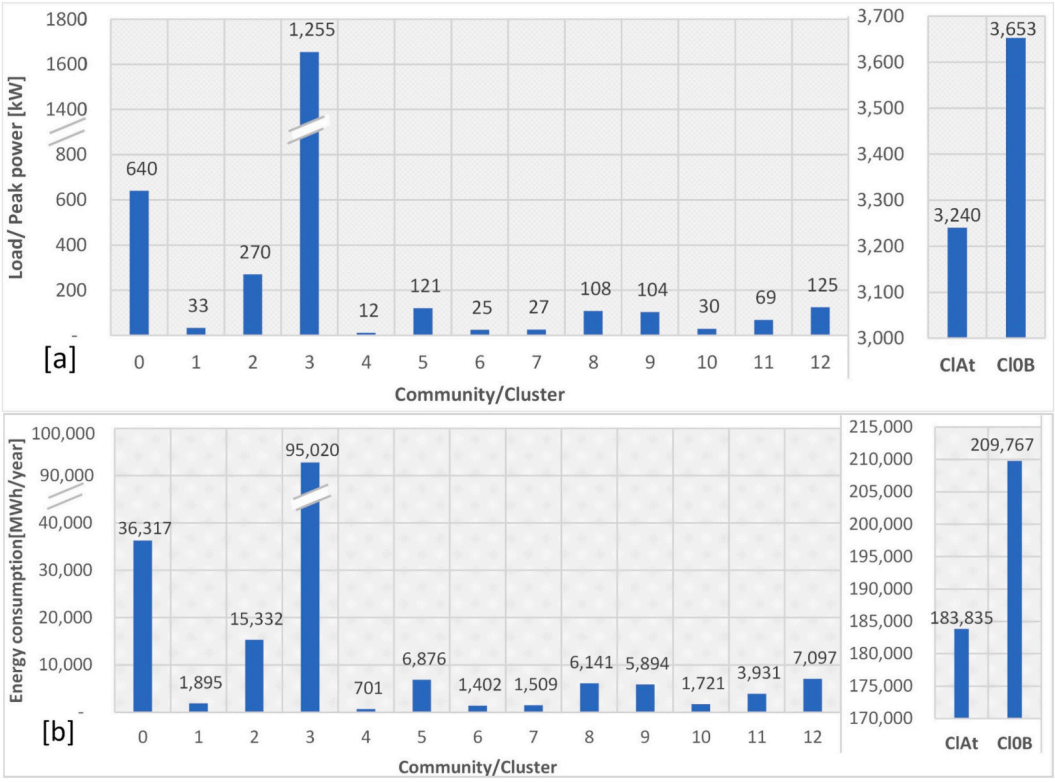

Fig. 8. Power peak values (a) and annual energy consumption (b) for communities in ClA (0−12) and Cl0B reference scenarios.

based off-grid generation sources or possibly among feasible community grids.

Internal grid routing design

Majaua-AP has a rudimentary grid routed through a three-phase MV line, expanded from the existing hydropower's main power transformer. The lines move through Majaua-Sede and Dachudua and use MV/LV PTs that drop power to a consumption level to feed a limited number of households. Similarly, in this study simulations followed a geospatial hierarchical network structure in which the procedure is defined for creating branch/feeders and collateral cables. The required input parameters are population threshold, set to consider a minimum of 65 and 5 people inside of each cluster's terminal nodes, and line base costs[5] of US$/km 9000 and 7000 for main branches and collateral lines, respectively. The grid layout details for ClA and Cl0B are illustrated in Fig. 9.

Comparing the grid layout details overlayed with the cost surface maps (Fig. 5b), shows how the terrain's topologies and the different Pf coefficients influenced the grid infrastructure investments. The

[5] Extracted from (MIREME, 2018) and excluding construction costs (labour, accessories).

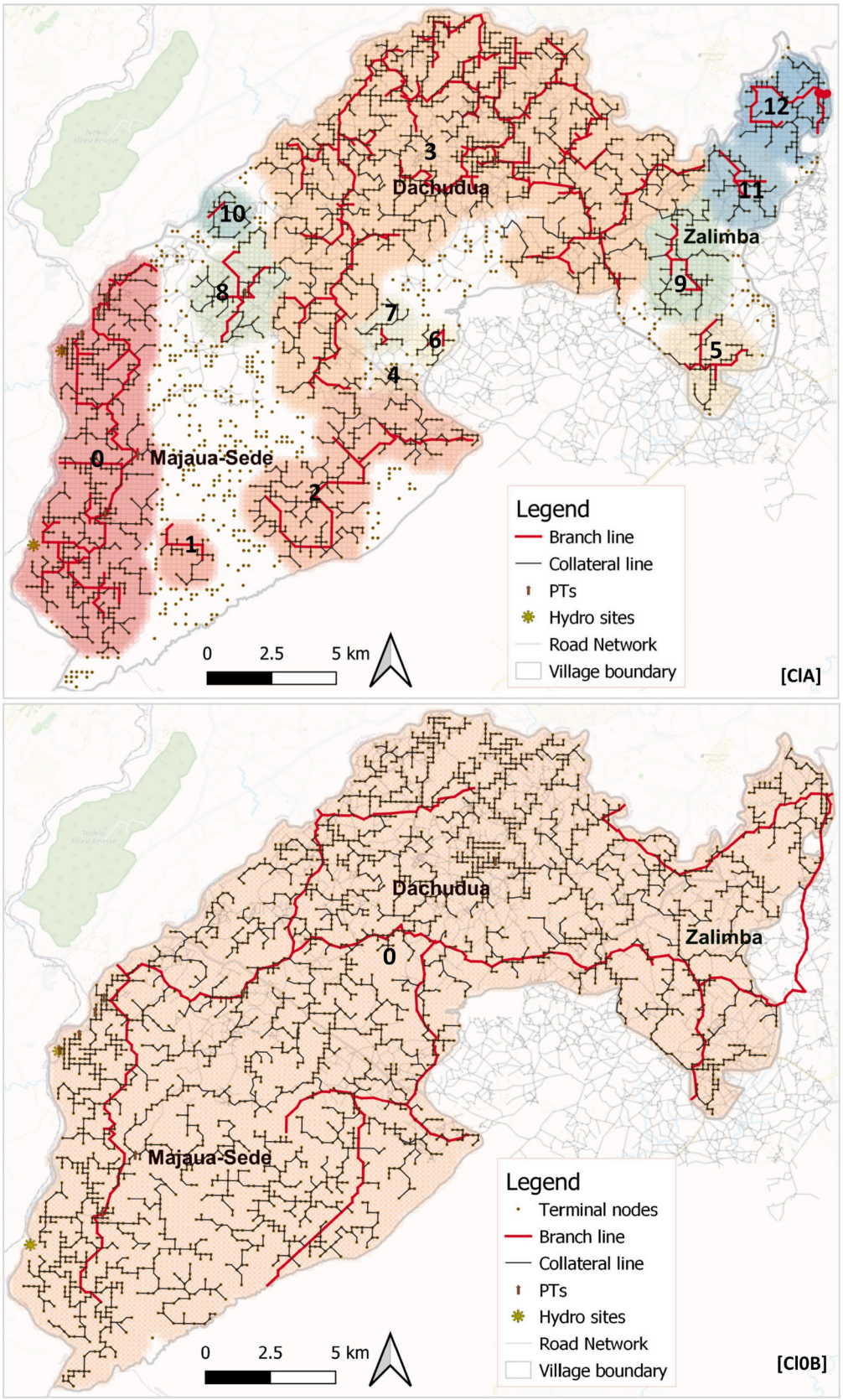

Fig. 9. Internal distribution grid routing within identified communities in ClA and Cl0B cluster strategies.

estimated least-cost paths (min NPC) for deploying lines also considered the operational and capital expenditures over the grid lifetime of 40 years. Table 2 presents the results of the population size, covered area, and related grid lengths and investments according to the line type.

By analysing Fig. 9, Fig. 5b and Table 2 show that communities with similar characteristics (eg. population size and covered area) are heavily affected by the Pf. On the one hand, community 1 (Pf: 8–9.1) whose size is 122 km^2 and grid cost US$k 552, compared to higher size communities 5, 8, 9, 11, and 12 (Pf: 3.7–5.8, size 229–334 km^2) their required grid investment is lower US$k 265–459. On the other hand, for community 0 (Pf: 6.9–8, size1,469 km^2), whose size is 3 times lower than community 3 (Pf:1.5–3.2, size 3681km^2), their total NPC for deploying lines are within similar cost range, i.e., US$k 4983 and US$k 5384 respectively. These outcomes demonstrate how the terrain peculiarities affect the cost-optimal results.

Furthermore, all communities do show potential (i.e., >100 kW) to be routed with a main branch MV connection. Community 3 (1655 kW demand) is economically viable to be connected to a NG if the connection line shows a least-cost solution. For the remaining communities in ClA, could be fulfilled through off-grid options. In addition, when considering the Cl0B strategy (Fig. 10, Cl0B), both main feeder and the collateral distribution grids were created. Among ClA communities, the internal grid lengths ranged from 4 to 383 km and 816 km in Cl0B, resulting in a total NPC of US$k 16,303 and US$k 19,156, respectively. Therefore, during the planning stage, planners should pay attention to these aspects when prioritisation decisions are taken.

Microgrid sizing: optimised electrification strategies-based scenarios

The techno-economic competitiveness analysis between each resulting hybrid microgrid configuration (wind/solar/hydro/diesel/storage) depends on local data availability, including estimated demands, RE source potentials, fuels, and the cost assumptions (Section "Developed scenario description"). Relying only on the estimated 627 kW hydropower capacity would not fulfil all the communities' energy needs. An additional assessment, implying system hybridisation with locally available energy sources was simulated under the developed scenarios (fixed demand in SCN0, and a linear load evolution in SCN1 and SCN2) through the MILP procedure and taking into account the technology cost-trend scenarios. The optimal hybrid microgrid generation portfolios and component capacity size installed in each community, including their annual power production, are presented in Fig. 10.

The analysis reveals that all the currently enabled technologies in GISEle (PV, HT, DG, and BESS), except WT, are selected. In SCN0, 75 % of the communities were suited to a 100 % share of RE-based hybrid component installations. A complete mix of RE technology configurations including diesel generators were installed in communities 0, 2 and 3. For communities 5, 9, 11 and 12, hydro played no role, instead of PV and BESS combinations were chosen. These communities are located out of the specified maximum river threshold range (15 km radius) and possible hydro installations. The installed capacities among communities under the ClA strategy range from 1 to 5155 kW (PV), 10–470 kW (hydro), 16–288 kW (DG), and 2–4840 kW (BESS), respectively, while for the single Cl0B strategy, the capacities range from 7361 to 10,004 kW (PV), 740–1160 kW (hydro), 640–656 kW (DG), and 28,910–39,878 kW (BESS) from SCN0 to SCN2, with an increased trend including on their related power production.

The procedure considered the installed capacities as distributed generation systems. The evolving demand patterns influenced the hybrid microgrid configurations and size to cope with current and future loads. Similar results are observed when simulations are performed over 15-year project timeframe. Clear influences are also visible in the share of DG among microgrid configurations when demand evolves from SCN0 to SCN2 where there is an increased trend in the mix of technologies, as summarised in Table 3.

Sensitivity analyses on cost scenarios

Effects of different project time horizons on the least-cost optimisation results

Fig. 11 shows the investment costs for electrifying community in terms of LCOE (Fig. 11A) and NPC (Fig. 11B), assessed over 10- and 15-year timeframes. In most instances, simulations yield significant LCOE reductions. Over a 10-year time –horizon, high LCOEs can be observed, especially in the fixed SCN0. However, taking averages as metrics, when growth is present, the average LCOE decreases from 0.226 to 0.190 US $/kWh considering10-year timeframe and with a significant decrease being observed over a 15-year timeframe, i.e., from 0.163 to 0.149 US $/kWh explained by the components' residuals (Petrelli et al., 2021).

Nevertheless, in all instances where the hydro is not installed (see Section "Microgrid sizing: optimised electrification strategies-based scenarios"), the LCOE is increased. This may be attributed to additional system costs fulfilled with BESS. Comparing the aforementioned results with key reports by IRENA and ESMAP, and despite our findings resulting in lower LCOEs these cost figures corroborate with the expected minimum average LCOE of 0.30 US$/kWh by 2025 for hybrid minigrid (IRENA, 2016) and 0.22–0.27 US$/kWh by 2030 (ESMAP, 2022).

The total investment cost per installed technology (Fig. 11B) is consistent with the previous findings. The reduced system configurations' capacity in SCN0, also entails a lower NPC with ranges from US$k 164 to US$k 7447. System configurations with a significant share of renewables (Fig. 10, SCN0) require higher investments due to reducing the DG along the entire time horizon. Furthermore, when capacity expansion under SCN1&2 is allowed, a slight increase in NPC occurs. Finally, the total investment cost for electrifying the identified communities (as for SCN1, Table 2, Fig. 10) is estimated to US$k 57,157 and

Table 2
Combined results of the clustering and grid routing procedure.

Community:	Population.	Size (km^2)	Branch length [km]	Branch cost [k$]	Collateral length [km]	Collateral cost [k$]	Grid length [km]	Total NPC [k$]
0	8546	1469	42	1250	111	3734	153	4983
1	446	122	3	205	6	346	9	552
2	3608	827	17	790	60	2504	77	3294
3	22,360	3681	113	1394	271	3991	383	5384
4	165	40	–	–	4	41	4	41
5	1618	238	6	88	11	176	17	265
6	330	64	1	31	4	69	6	100
7	355	92	1	22	6	102	7	124
8	1445	296	8	112	19	267	26	379
9	1387	334	5	80	18	272	23	352
10	405	92	1	16	7	90	8	105
11	925	229	4	60	13	204	17	265
12	1670	276	8	125	18	335	26	459
ClAt	43,260	7760	207	4173	548	12,130	756	16,303
Cl0B	48,712	10,249	115	1680	702	17,476	816	19,156

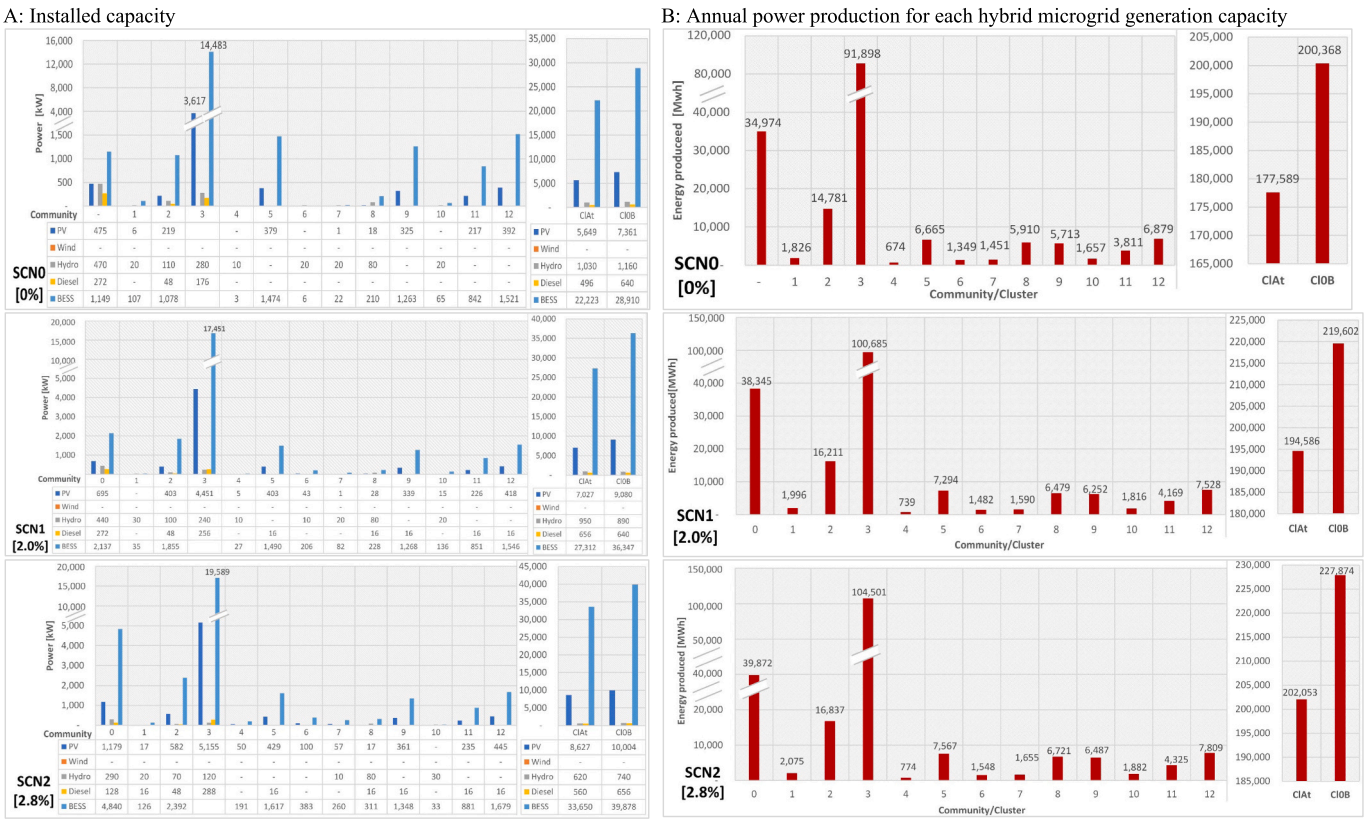

Fig. 10. Optimal generation portfolio of installed capacities (A) and the corresponding annual power productions (B) under the different growth scenarios among cluster ClA and Cl0B strategies.

Table 3
Off-grid hybrid microgrid component configuration share in each community-grid under the developed scenarios (10-year timeframe).

Hybrid microgrid technology configuration	Community/ SCN0	Community/ SCN1	Community/ SCN2
PV/Bess	5, 9,11,12	–	4,6
Hydro/Bess	4,6,10	1	10
PV/Hydro/Bess	1,7,8	4,6,7,10	7
PV/Diesel/Bess	–	5,9,11,12	5,9,11,12
PV/Hydro/Diesel/Bess	0,2,3	0,2,3,8	0,1,2,3,8
Hydro/Diesel/Bess	–	–	–

US$k 65,582 for ClA and Cl0B strategies respectively. This includes the internal distribution network. In the following sections, the discussions are drawn from SCN1 results.

Effects of diesel cost variations on the final microgrid configuration (installed capacity) results

A variable diesel price may influence the configuration of the system. Fig. 12 shows when the diesel price is decreased to 0.75 US$/l, the resulting system configuration increases the share of DG capacities. The opposite occurs when the diesel price increases up to 1.428 US$/l. In the Cl0B strategy, the required DG capacity is reduced from 2928 kW to 400 kW. Nevertheless, this variation only modestly affects the total system cost, which is kept close to the previous scenario patterns. However, the increased competitiveness of renewables leads to additional capacities on PV and BESS being required to sustain the system, hence affecting the overall system costs as shown in Fig. 11.

NPC analyses/integrated area optimisation & electrification strategy

In this final analysis step, the previous outputs on internal grid routing, and optimal microgrid generation portfolio capacities of each community are compared (in terms of their LCOE) with the possible NG connection points so that decisions on the final and best electrification strategies for the case area are proposed. However, despite not being identified in the study area, a demonstrative example is given with the assumption that a potential NG substation[6] would be deployed in Milange (already electrified) to expand the network to Majaua. In doing so, the local utility wholesale COE (0.143 US$/kWh) and the connection point details (location, available power and voltage level) are the considered input parameters. Next, the procedure is run in all scenarios to identify the optimal electrification strategy through connection paths either from the substation to the previously identified internal distribution community-grids or by keeping them as isolated microgrids or by sharing connections among them. The electrification expansion plan for Majaua is depicted in Fig. 13.

In this example the best electrification strategy is indicated as follows: Two community grids (0 and 3) were identified suitable for off-grid electrification hence the previous hybrid microgrid generation solutions are applied. In contrast, starting from the NG substation, a connection path (blue) connects communities 11 and 12 through a MV grid line. The remaining communities exploit intra-connections to them and between neighbouring communities based on their proximity and peak power values: i.e., community 12 connects9 while from community 11 it connects 5, 2, 4,7,6, 8, 1 and 10 respectively. The shape of connection paths is not straight as it follows the road network. The overall NPC costs on the best electrification strategies including connections and off-grid generation are summarised in Table 4. By using this approach, the total investment cost required for electrifying Majaua is estimated to US$k 39,557 and 6282 for off-grid and on-grid solutions

[6] NG point identified in collaboration with the local Utility staff .

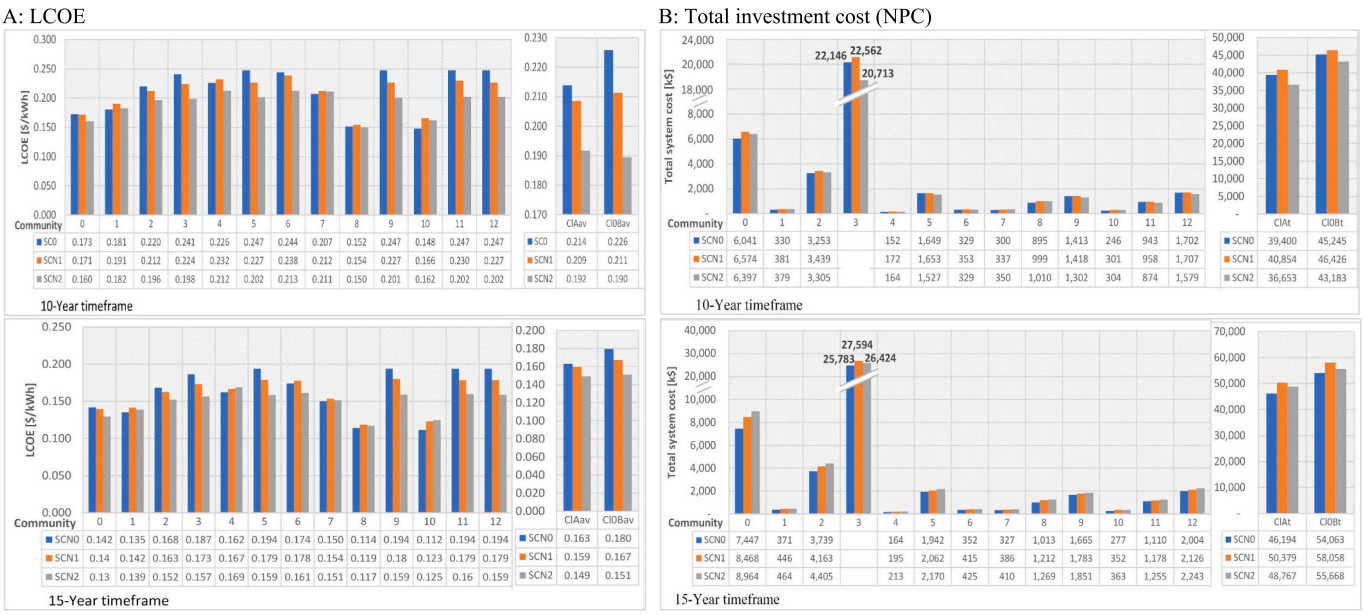

Fig. 11. LCOE (A) and related investments NPC (B) for each hybrid combination derived from model run among demand scenarios (SCN0 = no growth; SCN1 = 2 %; SCN2 = 2.8 %) evaluation within the short-to-medium term horizon. ClAav and ClBav are the average LCOEs considering the reference diesel cost (US$1/l) from ClA and Cl0B strategies respectively.

respectively.

The results allow for a village master plan to be developed based on the implemented approaches: first, by defining the priorities (e.g. socio-economic activities, population density, etc.) in the electrification project for system deployment to each community (ClA) or Cl0B strategy. This can be readily implemented step by step according to the resulting optimal off-grid microgrid generation portfolios NPCs and the financial resource availability. Secondly based on the NPC analysis results, the planner can decide the electrification pathways either to ClA or fulfil Cl0B, the whole administrative area. However, by comparing the total investment costs for electrifying the off-grid microgrid communities (ClA -US$k 57,157 and Cl0B-US$k 65,580) (Table 2, Fig. 11) with the NPC analysis results, it is evident that when grid connection is nearby located, the most convenient solution would be interconnecting to it.

Conclusion and next steps

This study, proposes an integrated geospatial modelling framework based on GISEle model, for optimisation of RE-based hybrid microgrids and network designs under uncertain conditions of rural energy systems, which most existing tools poorly addressed. Thanks to its open-source nature, the GISEle's wind and solar sizing capabilities was expanded by adding a hydropower option, including more sophisticated load demand assessments while simultaneously relying on free open-source tooling and tailored data.

The study analysis relied on the development of two community-based electrification expansion strategies (ClA&Cl0B) and three demand growth scenarios (SCN0-no growth-2025, SCN1–2030 (2 % growth), and SCN2–2035 (2.8 % growth), respectively) applied and demonstrated in a real rural setting in Mozambique and targeting planning the best electrification strategy based on cost-optimal technology mix either through off-grid hybrid microgrids and/or grid-connected. Depending on the project objectives, both alternatives chose either to go for a stepwise process of electrification where distinct individual communities are electrified sequentially over time (ClA), or immediately the entire area (Cl0B). The two expansion strategies are of great importance, especially for rural areas of developing countries where simply grouping the sparse structure of the rural population into single energy communities as required is not an easy task. Moreover, it helps make decisions on how to interpret the results and set electrification priorities according to their specific techno-economic implications and the available financial resources (Vinicius et al., 2021).

The scenarios went through all modelling procedures, from population clustering, grid routing, and microgrid sizing to NPC analysis with findings and decisions drawn on SCN1 results. The clustering analysis modelled 13 distinctive community-grids and a single entire community-grid. Due to the site specificities (terrain, population sizes, renewable potentials, fuel costs, etc.), each community has its requirements influencing the internal grid designs and the cost-optimal hybrid microgrid configurations. The enabled technology capabilities were considered in the analysis and chose to only disregard wind. This confirms the relevance of relying on off-grid HRES solutions, despite the electrification strategy enabling a connection to the grid when conditions exist, as exemplified in Section "Sensitivity analyses on cost scenarios".

The diversity of Majaua case findings also offers a clear scope for reflection by the stakeholders and scientific community. Firstly, power pick values among individual communities in ClA strategy varied from 12 kW to 1675 kW and 3653 kW considering the Cl0B. Secondly, in terms of the distribution grid, variety is also abundant. The overall line (branch and collateral) length is 756 km and 816 km for ClA and Cl0B strategies respectively. However, due to different terrain characteristics, the analysis also illustrates that the line costs can greatly differ, that is, the grid costs show no linear increase. As a concrete example, it can be seen that in community 0 (area 1469 km^2, grid line length 153 km) the final grid cost is US$k 4983. Thus, if these characteristics were ignored, the cost would be underestimated (3 times lower or more) at US$k 14,673. Thirdly, the modelled demand scenarios resulted in different hybrid microgrid configurations, i.e., the optimally installed capacities for each community increase as the demand evolves from SCN0 to SCN2 with diesel competitiveness mostly observed in SCN1. The SCN0 shows the highest share of RES, with 100 % RES share in most communities, namely 1, 7, 8, 10 (PV/Hydro/Bess), 5, 9,11 (PV/Bess), and 4,6 (Hydro/Bess). While demand increases (SCN1 to SCN2) the100%RES competitiveness decreases and DG is included in the mix in most community installations: 0, 2, 3, 8, 10 (PV/Hydro/Diesel/Bess) and 5, 9, 11,12 (PV/Diesel/Bess). It is worth noting that diesel comes into place for

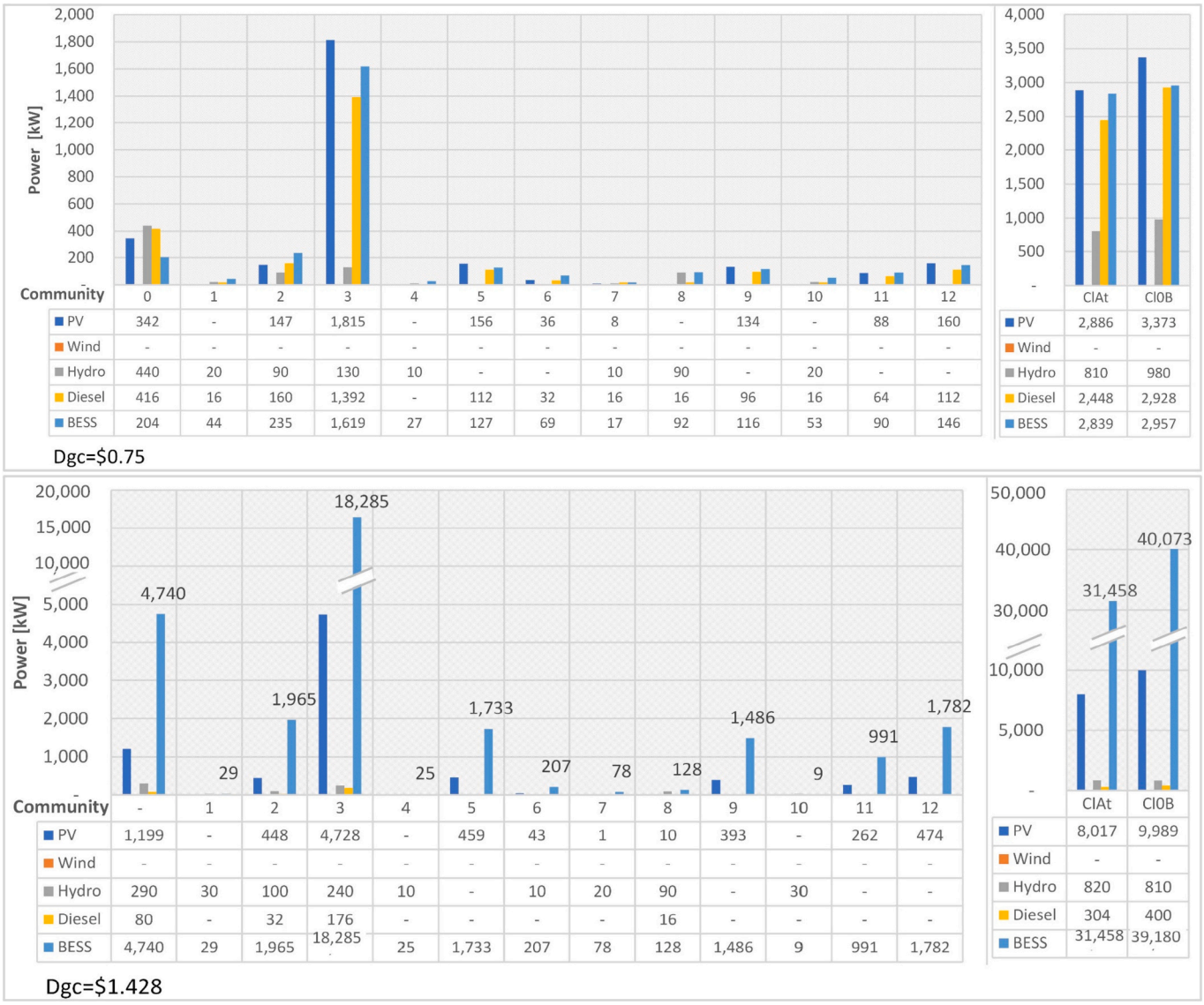

Fig. 12. Effects of diesel cost variation (0.75–1.428 US$/l) on the installed capacity and system configuration results.

community capacities above 124 kW, with RES share remaining below 100 %.

In terms of sensitivities, the LCOEs attributed to each integrated hybrid microgrid technology is a function of communities' characteristics. Comparing the results among demand growth scenarios, the LCOEs range varies from 0.148 to 0.247, with an average decrease as the demand increases. In addition, lower LCOEs is also observed when hydro installations are selected in the configurations. The project timeframe also influences the LCOE reductions, where lower LCOEs are observed in a 15-year timeframe scenario as shown in Fig. 12.

The analysis confirms that the developed modelling framework allows for an extensive analysis of multiple electrification strategies depending on the objectives set for electrification. The analysis also confirms that parameters' uncertainties deeply affect the design of the proposed hybrid microgrid system. However, by relying on scenarios, different electrification strategies, and sensitivity analyses, helps to highlight uncertainties and no-regret choices. In doing so, the tool provides a robust set of results to assist stakeholders (government and private energy utilities, academic, research, and international organisations) in planning cost-effective electrification solutions.

Therefore, the integrated methods presented in this study offer a set of innovative solutions to identify and define key priority areas towards sustainable and financially options at an early stage of rural electrification planning. Despite the obtained results for Majaua case being promising, this study also points to further developments and improvements to consider as follows:

- Upgrade the GISEle user interface to visualise the hydropower outputs, a process currently accessed through the dashboard output file;
- an important modelling challenge will be the addition of biomass resources as a potential energy generation source in the microgrid sizing procedure;
- automatise the inter-linked modelling procedures addressed in this study; and
- test and validate the tooling in other cases with different socio-economic, geographical, and climatic circumstances.

CRediT authorship contribution statement

Berino Francisco Silinto: Methodology, Data curation, Conceptualization, Writing – review & editing, Writing – original draft. **Darlain Edeme:** Software, Methodology. **Silvia Corigliano:** Software, Methodology. **Aleksandar Dimovski:** Software, Methodology, Writing – review & editing. **Christian Zuidema:** Supervision, Resources, Writing –

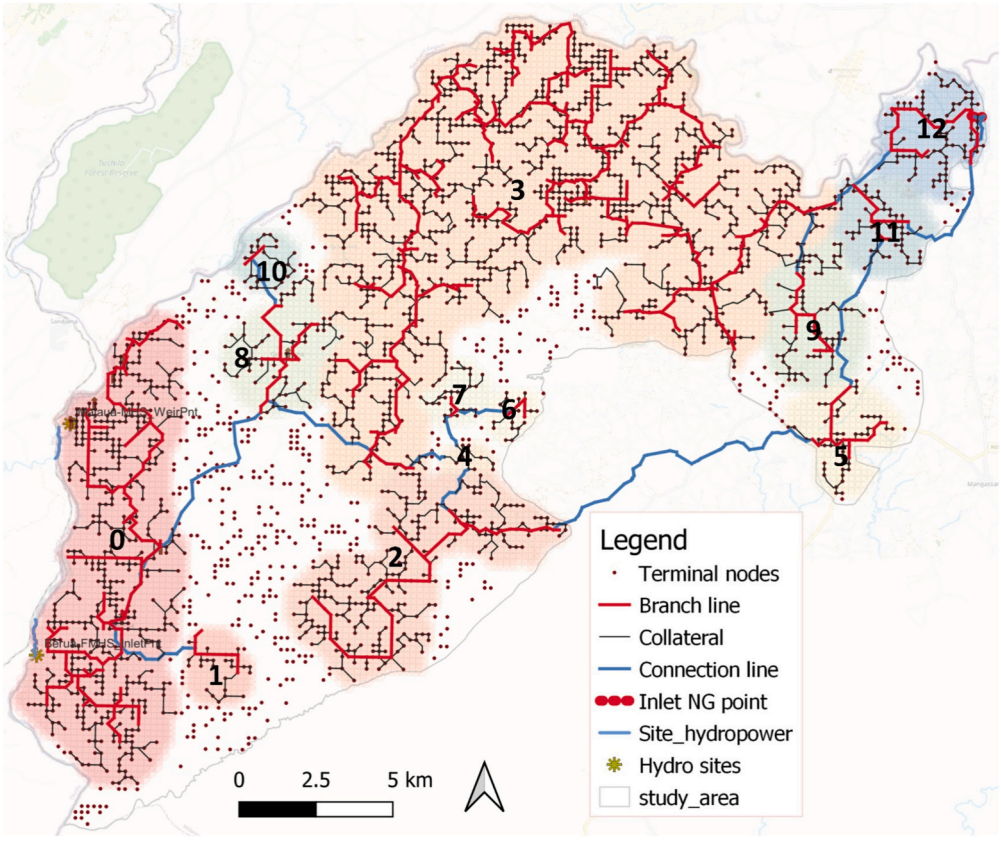

Fig. 13. Results of the NPC analysis and integrated area optimisation.

Table 4
Results of NPC/integrated area optimization analysis: electrification strategy.

Electrification strategy	Population electrified	Power peak [kW]	Connection length[km]	Connection NPC [k$]	Community/ connection type	Intra community grid length [km]	Intra community grid length NPC[k$]	MG cost NPC[k $]	Internal grid length [km]	Internal grid NPC [k$]	Total System cost NPC[k $]
Off-grid hybrid microgrid generation	8546	640	–	–	0	0	0	6574	153	4983	11,557
	22,360	1674	–	–	3	0	0	22,562	381	5438	28,000
NG expansion	3057	229	0.4	5	12 to 9	5.8	61	0	49	811	877
	165	696	6.6	58	11 to 5,2,4,7,6,8,1,10	43.8	489	0	153	4858	5405

review & editing. **André Faaij:** Supervision, Methodology, Writing – review & editing. **Marco Merlo:** Writing – review & editing.

Declaration of competing interest

The authors declare that they have no known competing financial interests or personal relationships that could have appeared to influence the work reported in this paper.

Acknowledgements

This research work is part of a PhD Scholarship programme developed within the framework of the Netherlands Initiative for Capacity Development in Higher Education (NICHE) project, entitled "Innovative ways to transfer technology and know-how, developing skills and expertise for gas, renewable energy and management" (NICHE-MOZ-231/263), funded by the Government of the Netherlands and administrated by the Dutch organization for internationalisation in education (Nuffic), grant number CF10792. Special thanks go to the Energy4Growing team for their continuous support of our project. The authors also acknowledge Castro Soares, a former PhD at Politecnico di Milano for providing support with the RAMP modelling tool.

Appendix A. Cost surface creation

The cost surface layer is created to represent the costs of building electric lines and is associated to the generated penalty factors containing specific deployment costs applied in the grid routing procedure (Step 2) (Corigliano et al., 2020; Vinicius et al., 2021). The weights of the calculated distance to the nearest road are modelled as a linear curve with a maximum of 6 points considering >1 km. The slope factor exponentially returns to 1 (doubling the cost) at 35 degrees. Each terrain type is defined based on the GLC2000[7] JRC project and a maximum Pf of 9.9 is assigned for water bodies. Moreover, higher weights are also attributed when the grid network is deployed at longer distances from roads, higher slopes, and extreme environments (e.g. rivers, dense forests, etc.). The coefficients are later multiplied by the resulting cost of the optimised electric line length times the base cost per kilometre [$/km] (Corigliano et al., 2020).

Table A.1
Penalty factors used for the cost surface determination in (Corigliano et al., 2020).

Constraint factors	Road distance [m]			Land cover			Fault/slope	River		Water bodies& lakes		Protected areas[a]	
Type/class	<100	>100 < 1000	>1000	Grass-Open forest	Tree cover shrubs	Closed forest	–	Yes	No	Yes	No	Yes	No
Penalty factor	0	Linear	6	1	2–4	5–8	Exponential	9	0	10	0	99.999	0

[a] Cultural heritage sites; vegetation coverage (natural parks, meadows and trees).

Appendix B. Load demand modelling and assessment

Table B.1
The main input parameters considered in RAMP model.

Parameters/dimensions	Description	Unit (range) measure
$User_j$	Category name of each user class j	User Type
N_j	Number of users within a specific user class j that owns specific appliance(s)	0-n
$Appliances_{,j}$	Name/and type of appliance owned by each user in a class j	Appliance type
n_{ij}	Number of appliances of type i within class j	0-n
P_{ij}	Nominal power absorbed by specific appliance(s)$_i$ of user	0-20 k [W]
fw_{ij}	Number of functioning window times: periods during the day that each appliance of a specific user$_j$ can be switched on	1–3
$W_{f,n}$	Start and end times of appliance's use during the day	0:00–23:59
Rfwij	% of random variability of daily functioning time allowed in a defined functioning cycle	0–100 [%]
ft_{ij}	Daily functioning time: total time the appliance is used (kept switched on)	0–1440 [min]
fc_{ij}	Minimum time of the functioning cycle the appliance ij is kept on after switch-on	
Rfc_{ij}	% of random variability of daily functioning time allowed in a defined functioning cycle	0–100[%]
fc_{ij}	Minimum time of the functioning cycle the appliance ij is kept on after switch-on	0–1440 [min]
	Constraint factor for the appliance usage specifically on weekday or weekend periods	We/wd/none

Appendix C. Key customisations, additions, and integration made to GISEle framework

As previously highlighted, in this study, out of hydropower potential assessment, wind and solar energy resources derived from global reanalysis models and satellite observations are openly available in online global databases including in renewable Ninja and within GISEle's microgrid sizing procedure in yearly power profiles. Doing so, Fig. C.1, reports the generated power profiles. Fig. C.1a depicts the hourly direct solar radiation while Fig. C.1b, the hourly wind power curves of the Majaua area. From September to March is the summer and rainy season in Mozambique where long periods of cloudy days may influence the reduction of solar radiation. In terms of wind resource potential, the average wind speed in this region is below 4.33, consequently lower than the cut-in velocity of the selected power turbine during most of the months of the year. Therefore, the option for its exploitation is probably not profitable for investment in power with such technology.

[7] Global land cover database for the year 2000

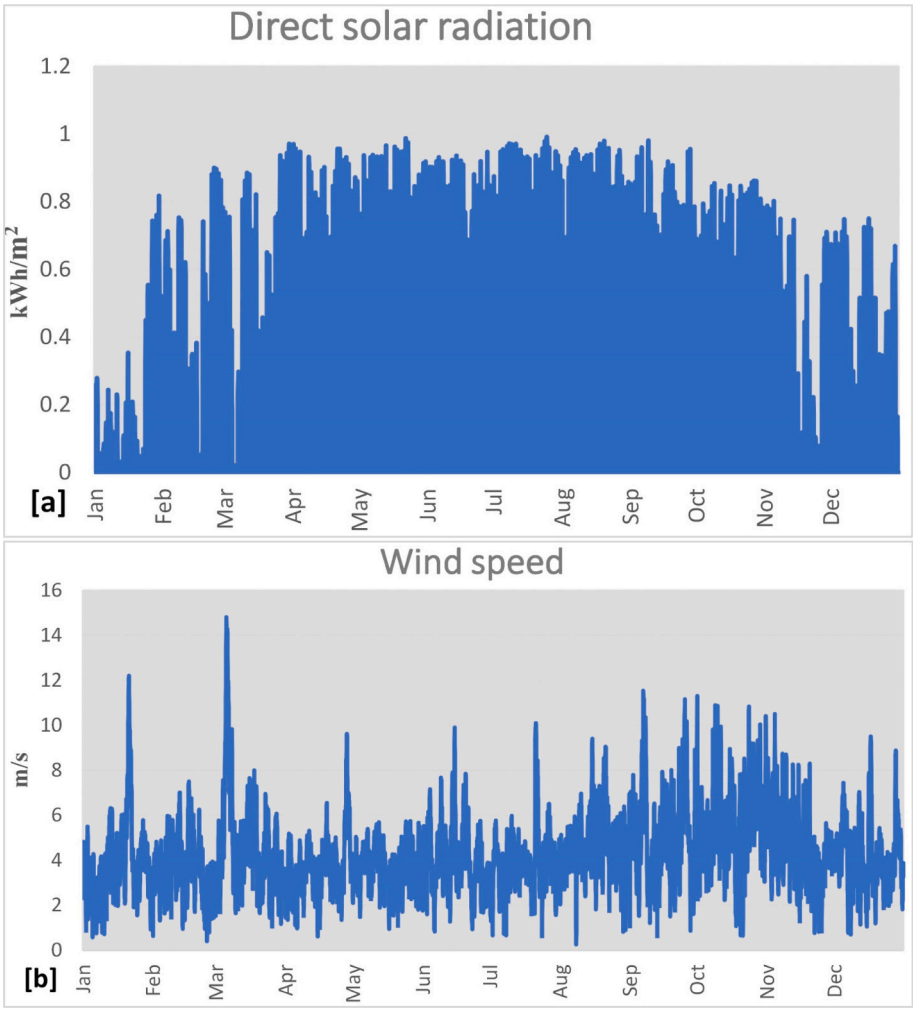

Fig. C.1. Direct solar radiation (a) and wind speed (b) of Majaua study area, 2019.

The estimation of hydropower resource potentials is the most challenging task. For such purposes, the SWAT+ tool is applied to watersheds (Moiz, Kawasaki, Koike, & Shrestha, 2018; Neitsch, Arnold, Kiniry, & Williams, 2011) to first assess and estimate the river flow rates and further interlink it to the GISEle framework. The SWAT + model is a physically hydrological model based on water balance principles and simplifications of the hydro-geologic cycle that combines geospatial data on elevation, land cover, soil, and weather patterns to allow a detailed description of the different processes contributing to the runoff formation in large and complex watersheds (Hasan & Wyseure, 2018; Neitsch et al., 2011). SWAT+ comes as plugin integrated into QGIS[8] environment as QSWAT+. It was developed by the United States Department of Agriculture (USDA) (Arnold et al., 1998) and is widely used to assist watershed managers in quantifying the impact of different land properties and management practices in large and complex watersheds (Boithias et al., 2017; Nkhoma, Ngongondo, Dulanya, & Monjerezi, 2021). The SWAT+ workflow including the pre-processing interlink feature to GISEle framework comprises 4 steps depicted in Fig. C.2 and summarised below:

[8] QGIS Quantum Geographical Information System

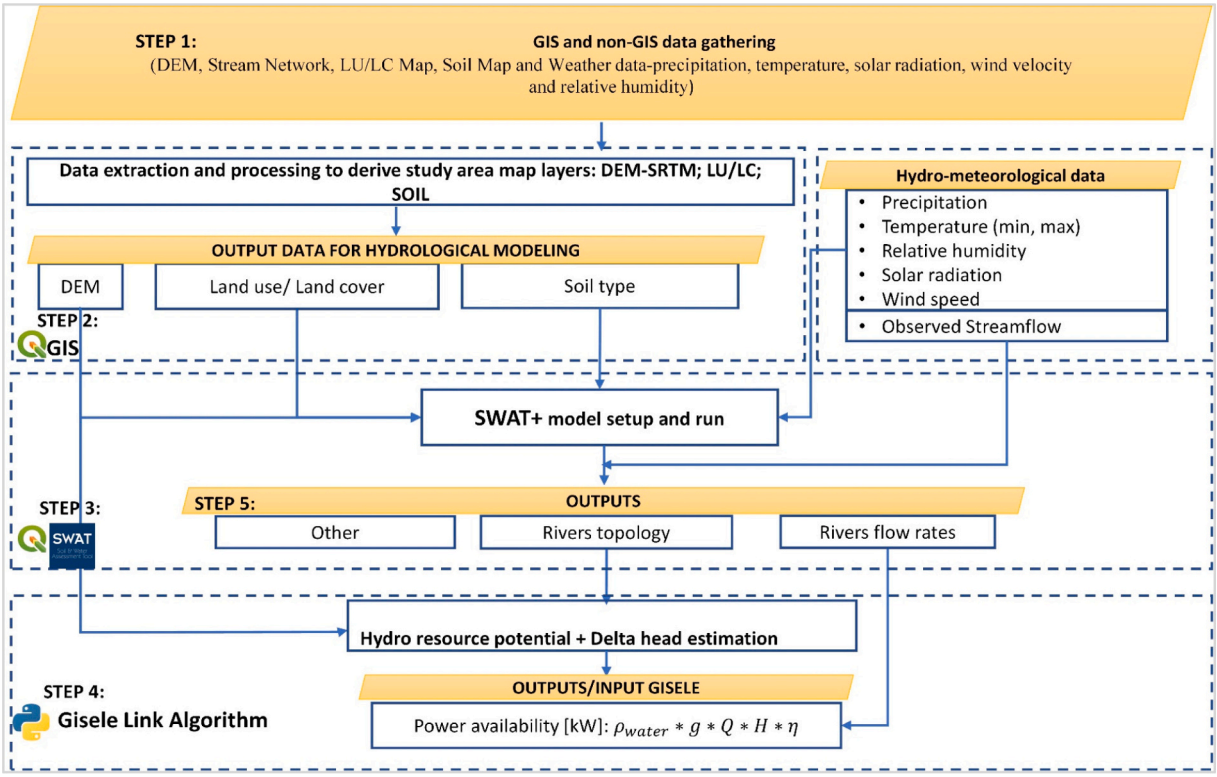

Fig. C.2. A workflow of the SWAT/hydrologic model to estimate river flow rate and the output to link with GISEle for hydro-power potential assessment.

Starting from the data gathering all the required data (Step 1) for set-up the QSWAT+ hydrological modelling is processed in Step 2 following the procedures addressed (Silinto, Edeme, et al., 2025) SWAT+ is based on the concept of Hydrologic Response Units (HRUs)representing layers/areas with a unique combination of landscape unit (LSU), soil and land use maps, and slope classes maps describing the spatial heterogeneity within a given watershed. Climate data is also required (Table C.1). SWAT+ used the LSU to discretise subbasins and allow the separation of upland processes from wetlands. During model setup, step 3, subbasins are delineated based on stream thresholds while LSUs are delineated based on channel thresholds as described in the user manual (Dile, Srinivasan, & George, 2022). Decision tables are introduced to schedule activities that are only carried out when specified conditions related to land-use management and reservoir management are met.

Table C.1
List of GIS & non-GIS input datasets used in SWAT model for the hydrological assessments.

Dataset	Description	Source
Basin & administrative boundaries	Vector layer-polygon	(GADM, 2022)
Land use/cover project definitions	Raster layer-10/30 m: including10/22land use/cover types	USGS/Geospatial Information Agency
Elevation	Raster layer-30 m: NASA SRTM Digital elevation/slope	(Jarvis et al., 2008)
Soil type	Soil type/ raster1:25000/7 km	FAO/https://daac.ornl.gov/
Global River Network (HydroSHEDS)	Vector layer - Polyline	https://www.hydrosheds.org.gov (Lehner, Verdin, & Jarvis, 2008)
Global Streamflow Characteristics Dataset (GSCD)	Raster	(Beck, de Roo, & van Dijk, 2015)
River discharge	River flow [m^3/s] 1station (monthly, 2009–2012)	Water Resources Agency of Malawi
Precipitation	Daily precipitation [mm](.txt)-9 stations (2006–2013)	Water Resources Meteorology Agency of Malawi and Mozambique; Global weather SWAT database (Roth & Lemann, 2016)
Temperature	Minimum and maximum temperature [^oC] (.txt)	
Relative humidity	Fraction [%] (.txt)-2 stations (2006–2013)	Global weather SWAT database (Roth & Lemann, 2016)
Wind speed	Average daily wind speed [ms^{-1}]-(.txt)	
Solar irradiation	Average daily [MJm^{-1}]-(.txt)	

Therefore, the model run starts by choosing the hydrological basin study area and the outlet point which consists of all water streams flowing from its tributaries. In this process, the 30 m resolution DEM raster input layer of the river basin area is used to identify and delineate the existing watersheds, which in turn are subdivided into sub-watersheds (sub-basins) (Dile et al., 2022), connecting them through several streams and river network flow directions (set by a minimum threshold of 200–500 m). In a further stage follow the integration of Soil and land use maps of the sub-watershed area previously developed and lately spatially distributed into multiple HRUs for each basin. In the sub-basins, each corresponding accumulated river flow rates are computed and combined with the available climate data to provide information on the hydrology patterns of the basin area, including

the total river flow discharges as output. Once the inlet/outlet point the expected simulation results are routed through a stream network derived from the DEM to the stream outlet where we have a simulated and an observed flow. These flows are compared and adjusted (through their interrelated parameters) to the best match.

Depending on the desired model configuration the river flow discharges are provided at daily, monthly, and yearly average basis following the time-series of available climate data (Dile et al., 2022). At the final stage, SWAT+ applies a user-specified method for estimating potential evapotranspiration (Priestly-Taylor, Penman-Monteith, and Hargreaves) (Neitsch et al., 2011) combined with the rainfall time-series data to simulate and estimate the daily flow/runoff, sediment yield, and other parameters for each HRU. For multiple inlet points, an iterative procedure is applied by accumulating estimated water flows at the sub-basin level (Arnold et al., 1998; Neitsch et al., 2011). Further, the hydrological modelling processes are computed using the simplified (from the hydrogeologic cycle) water balance Eq. C.1 (Dile et al., 2022; Neitsch et al., 2011) from which the model provides the average (daily, monthly, and yearly) river discharges covering all the simulated years. The discharge output is subsequently calibrated using the SWAT+ model or SWAT+ toolbox.

$$SW_t = SW_0 + \sum_{t=1}^{t=n} (R_i - Q_{si} - E_i - W_i - Q_{ri}) \quad (C.1)$$

where, SWt represents the final soil water content [mm], SW0 the initial soil water content on day t [mm], t the time [days], Ri(day) the amount of precipitation on day t [mm], Qri(surf) the amount of surface runoff on day t [mm], Ei the amount of evaporation and transpiration on day t[mm], Wi (seep) the amount of percolation and bypass through the bottom of the soil profile on day t [mm], and Qri the amount of return flow on day t [mm].

The hydropower potential is computed in (Step 4) using the Python algorithm through which the river flow discharge output from the SWAT+ model is used as input in GISEle. This algorithm uses the DEM layer of the watershed area and follows the simulated river stream including its branches, along which the available average head[9] is computed with unique river flow discharges (without inlet or outlet flow). With this combination, the hydro resource potential is computed considering the average power profile availability of the closest rivers associated to each community-specific distance (set above a certain threshold). Subsequently, the estimated amount of hydropower potential P(t) is computed using the Eq. C.2:

$$P(t) = Q(t)*\rho*g*H*\eta \quad (C.2)$$

where ρ is the density of water [kgm^{-3}]; g is the gravitational acceleration [9.8 ms^{-2}]; Q(t) is the dependable monthly average river flow discharge [m^3s^{-1}]; H is the available head (height difference) or elevation drop [m]; and η is the hydro turbine efficiency [0.8].

In this study, the estimated river flow discharges were generated using a simulation period of 34 years (from 1981 to 2013) and a warming period of 2 years. The process used rainfall data measurements gathered from 1 river gauge (M1-Roadbridge/Malawi) and adapted to the simulated model parameters to fit the available datasets and obtain the estimated river flow discharges for Majaua. Fig. C.3 shows the estimated river flow results after running the SWAT+ procedure and its link to GISEle+. Fig. C.3a illustrates the annual hydropower potential over the watershed basin and Fig. C.3b the average monthly flow rate curve. The Ruo river stream flaws at a constant regime during the whole year, with high discharge rates being observed during the rainy season months (December–March). The waterfall flow and net head is situated at an elevation of 460 m above mean sea level. Seasonally, the river flow high picks occur from Jan-March with a pick value of 193.1 m^3s^{-1}in February during the summer and rainy season, and lower values from April to October, with the lowest of 2.2 m^3s^{-1}; in September. These patterns highlight the dependence of the rivers' flow rates on the rainfall regime, where during winter and dry months/season the power potential is significantly reduced. The resulting values are in line with the unsystematic recorded datasets, gathered during the field surveys, which are at least comparable with historical river flow rates, measured at the station (Bridge). The estimated hydropower potential set in the localised mini-hydro site is 627 kW.

[9] Heads along the river are computed using DEM layer based on a linear regression model along the branch of the river sampled at each 100/200 m elevation length, here considered reasonable for derivation channel of run-of-river hydro turbines.

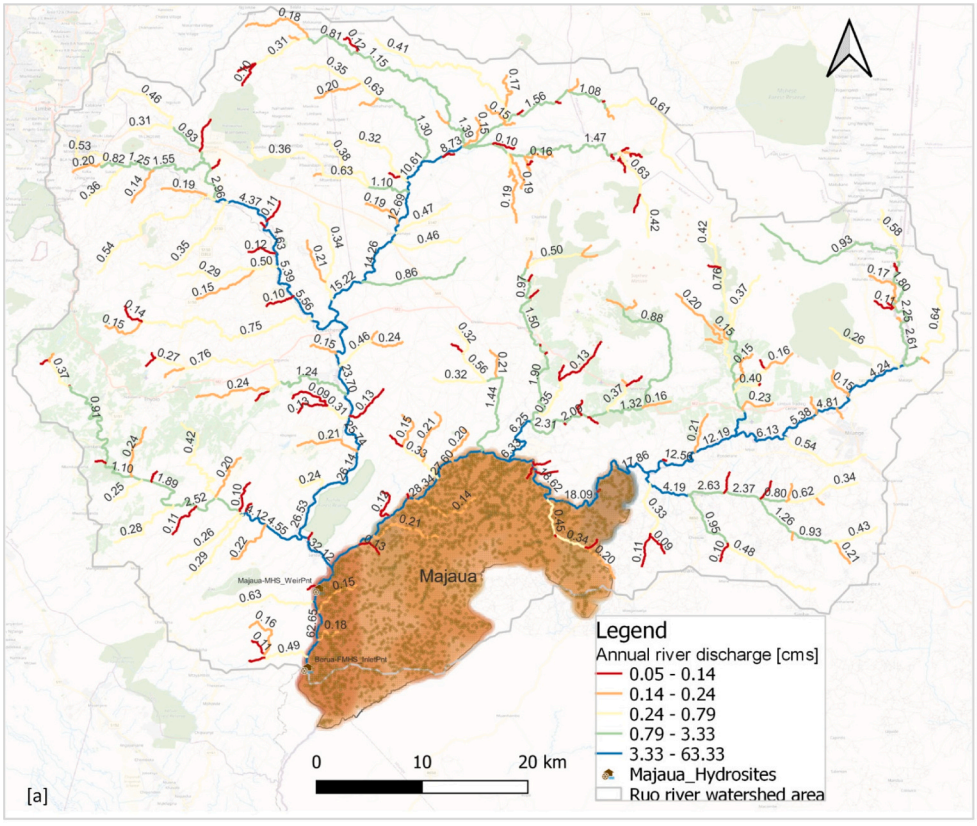

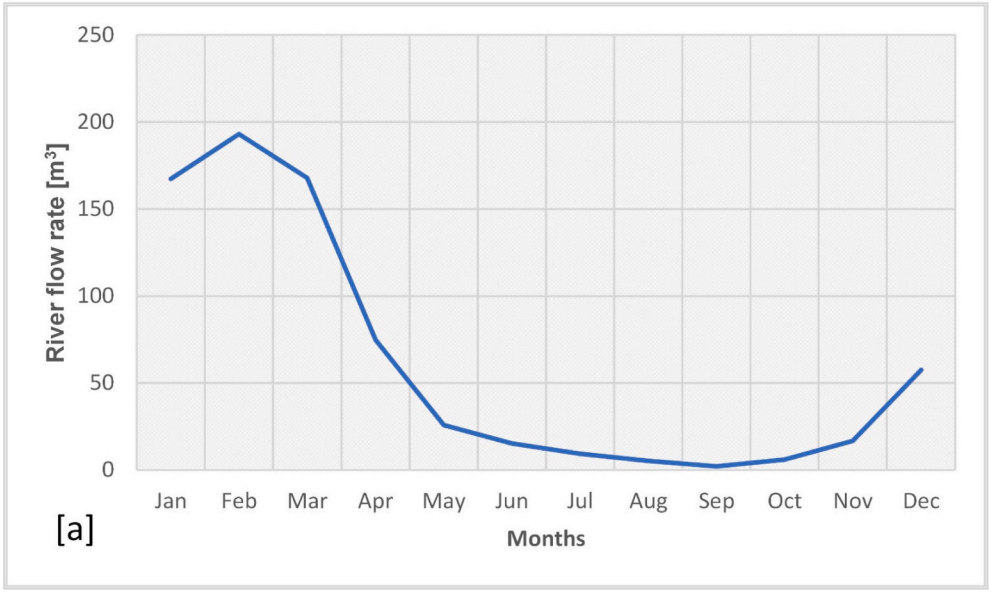

Fig. C.3. Average annual (a) and monthly (b) river flow discharges derived from SWAT+ modelling outputs over Ruo River watershed basins.

Appendix D. Techno-economic data used in this study

Table D.1
System components and cost assumptions used in the scenario analysis (microgrid sizing module).

System components	Capital cost [$/kW]	O&M [$/year]	Lifetime [years]	Efficiency [%]	Avg. capacity factor	Scenario/years
PV System (DC) 1 kW	1378	10	25	1	0.3	SCN0/2025–2025
PV System (DC) 1 kW	984	10	25	1	0.3	SCN1/2025–2030
PV System (DC) 1 kW	886	10	25	1	0.3	SCN2/2030–2035
Hydro turbine [<1000kWAC]	1800-8000	40	25–50	0.8	0.68	All
Wind turbine150kW	1489	540	25	1	0.18	SCN0/2025–2025
Wind turbine150kW	1191	540	25	1	0.18	SCN1/2025–2030
Wind turbine150kW	1087	540	25	1	0.18	SCN2/2030–2035
DG [16 kW]	12,000	1752	750		0.3	All
Li-ion [kWh]	400	10	15	0.975		SCN0/2025–2025
Li-ion [kWh]	388	10	15	0.975		SCN1/2025–2030
Li-ion [kWh]	326	10	15	0.975		SCN2/2030–2035
Converter	420	0	15	95	0.3	All

Table D.2
Summary of electrical parameters and costs [US$] assessed.

Data	Value	U.m.
Grid line investment cost (branch & collateral)	9000 & 7000	[$/km]
Grid lifetime	10–40	[Years]
COE	0.143	[$/kWh]
Power transformer (800kVA) cost[a]	15,700	[$]
Diesel cost (range scenario assumptions)	0.75, 1.00[b], 1.43	[$/l]

[a] PT for connection point assumption.
[b] Reference cost.

Table D.3
Reference techno-economic index parameters and variables applied in microgrid sizing and NPC analysis procedures.

Parameter	U.M	Ass. value
Cost of fuel	[$/l]	1
Project lifetime	[years]	10
Number of typical days	[day/year]	12
Maximum energy not supplied	[%]	5
Minimum energy produced by RES	[%]	0.8
Cost coefficient for DG	[l/h]	
Cost coefficient of DG	[l/h/kW]	
Load forecast error	[0–1]	0.1
PV forecast error	[0–1]	0.1
WT forecast error	[0–1]	0.25
Project discount factor	[0–1]	
Interest rate	[0–1]	0.06
PV modules		
Unitary capacity	[kW]	1
Capital cost	[$/unit]	1378
O&M yearly cost lifetime	($/unit/y][years]	1020
Wind turbine		
Unitary capacity	[kW]	150
Capital cost	[$/unit]	27,000
O&M yearly cost lifetime	($/unit/y]	540
Lifetime	[year]	20
Diesel generator		
Unitary capacity	[kW]	16
Capital cost	[$/unit]	12,000
O&M yearly cost lifetime	($/unit/h][hours]	0.215000
Cost coefficient	[l/h]	0.4672
Cost coefficient	[l/h/kW]	0.3
Min power of DG	[0–1]	0.3
BESS		
Unitary capacity	[kWh]	1
Capital cost	[$/unit]	400
O&M yearly cost	[$/unit/y]	10
Lifetime	[kWh]	3000
Lifetime	[H]	15
Efficiency	[0–1]	0.975

(*continued on next page*)

Table D.3 (*continued*)

Parameter	U.M	Ass. value
Maximum BESS power-to-energy ratio	[kW/kWh]	1
Maximum BESS depth of discharge	[0–1]	0.9
Hydro turbine		
Unitary capacity	[kW]	10–1000
Capital cost	[$/unit]	80,000
O&M yearly cost	[$/unit/y]	0.36
Lifetime	[years]	40
Min Power of HT	[kW]	0.5
Efficiency		0.8
max_ht_power		1000
Min ht_power		10
max_ht_units		1000
max_ht_dist	[m]	15,000

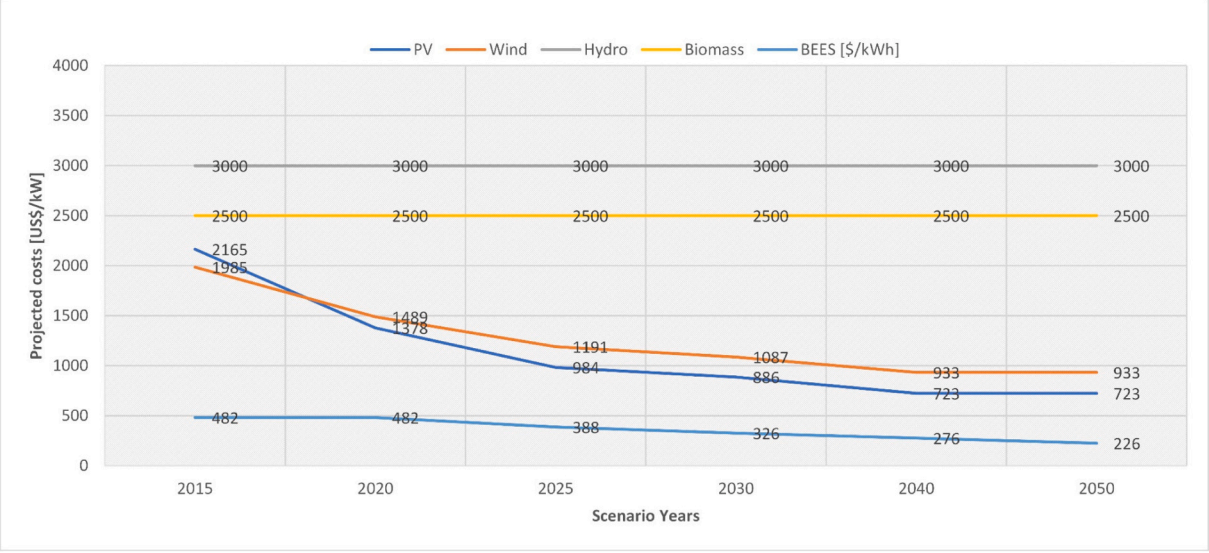

Fig. D.1. Cost trends of selected PV, Wind, Hydro, and Biomass renewable technologies including batteries up to 2050. Plotted by the first author using data from reference (Allington et al., 2023; Cole & Frazier, 2023).

Appendix E. Clustering and load demand assessment

Clustering procedure: As previously highlighted in Section "Applying the improved GISEle-based framework", Step 1, clusters can be formed by points that fulfil the user requirements to have at least "MinPts" points in a radius of "eps" values chosen after performing a sensitivity analysis in the clustering procedure. However, by focusing on the first row for eps = 1000 depicted in Table E.1a and starting from the lowest "MinPts" means that many points are classified as "core" points that can be merged to form clusters. In this study analysis the number of clusters can increase from 1 up to 17 by using MinPts = 100 and 442 respectively. This procedure, results 1 cluster covered by 99 % people and 17 clusters covering 73 % of people of the study area (Table E.1b). Further, by increasing MinPts to 214, 328, etc., 2 and 13 clusters are identified but also results 2 % and 12 % outliers respectively. This behaviour is simply because this increase acts as an additional filter that created outliers, effectively by splitting the large cluster in two because all the core points are not in the desired radius anymore.

Table E.1
Sensitive analysis results on best combination of Ɛ-eps and MinPts parameters for DBSCAN/cluster analysis: Result based on the total number of clusters (Table E.1a), percentage of clustered people (Table E.1b), Number of people in the area (Table E.1c).

Table E.1a: Number of clusters

MinPts / *ε-eps*	100	157	214	271	**328**	385	442	500
1000	1	1	2	6	**13**	11	17	14
1285	1	1	1	1	1	1	1	4
1571	1	1	1	1	1	1	1	1
1857	1	1	1	1	1	1	1	1
2142	1	1	1	1	1	1	1	1
2428	1	1	1	1	1	1	1	1
2714	1	1	1	1	1	1	1	1
3000	1	1	1	1	1	1	1	1

Table E.1b: Percentage of clustered people

MinPts / *ε-eps*	100	157	214	271	**328**	385	442	500
1000	99	99	98	94	88	81	73	63
1285	100	100	100	100	100	99	98	97
1571	100	100	100	100	100	100	100	100
1857	100	100	100	100	100	100	100	100
2142	100	100	100	100	100	100	100	100
2428	100	100	100	100	100	100	100	100
2714	100	100	100	100	100	100	100	100
3000	100	100	100	100	100	100	100	100

Table E.1c: Number of people in the area

MinPts / *ε-eps*	100	157	214	271	**328**	385	442	500
1000	119	120	122	130	139	150	164	173
1285	119	119	119	119	119	120	122	124
1571	119	119	119	119	119	119	119	119
1857	119	119	119	119	119	119	119	119
2142	119	119	119	119	119	119	119	119
2428	119	119	119	119	119	119	119	119
2714	119	119	119	119	119	119	119	119
3000	119	119	119	119	119	119	119	119

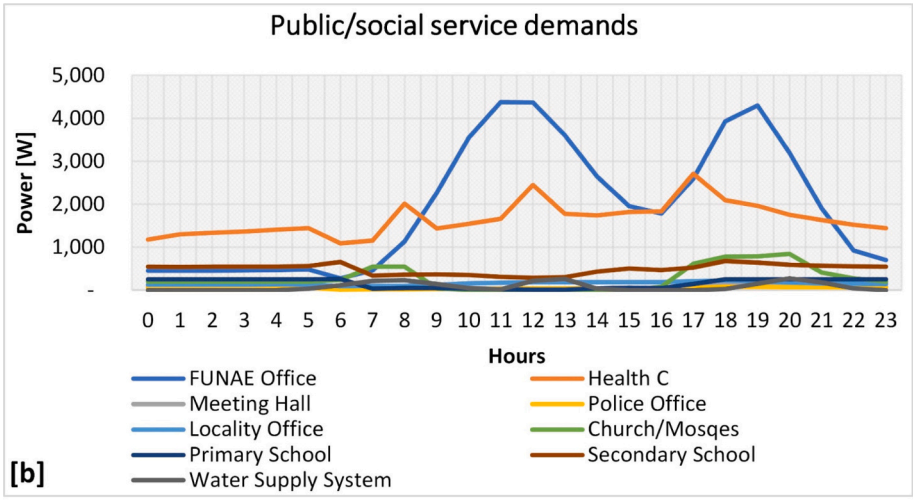

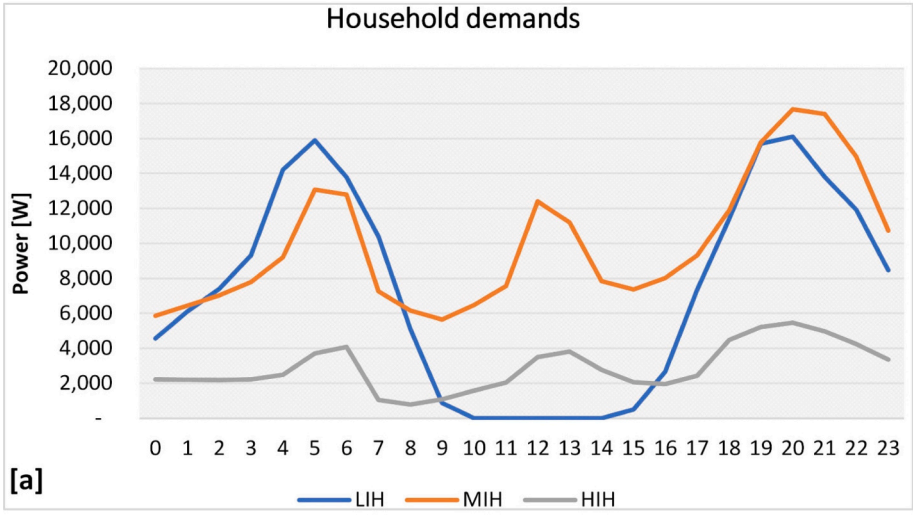

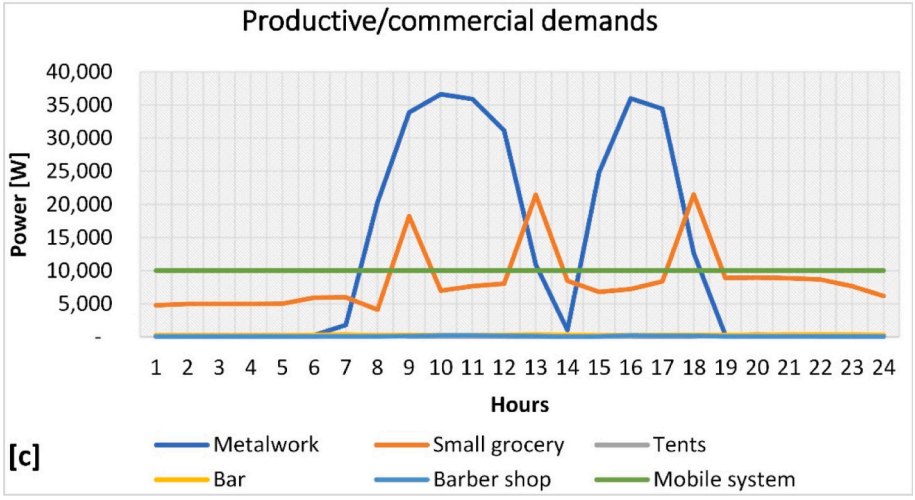

Fig. E.1. Daily load demand profiles disaggregated per user type within each demand category: Households (low (LIH), medium (MIH), high (HIH) income households) (a), social (b) and productive/commercial (c) representative for Majaua AP.

Table E.2
Ramp input data & coded parameters.

A: Household

$User_{ij}$	N_j	$Appliance_{ij}$	n_{ij}	$P_{i\,j}$ [W]	Fw_{ij} [1,2,n]	Ft_{ij} [min]	Rft_{ij} [%]	Fc_{ij} [min]	StartW1 [min]	EndW1 [min]	StartW2 [min]	EndW2 [min]	StartW3 [min]	EndW3 [min]	$Rfw_{i\,j}$[%]	Year Min
LIH	302	Lights Outdoor	1	25	2	780	0	780	0	420	1050	1440	–	–	0	–
		Lights Indoor	2	20	2	660	0.15	10	240	480	1080	1440	–	–	0.25	–
		Phone Charger	1	7	2	300	0.2	60	1080	1440	0	420	–	–	0.35	–
		Radio	1	10	2	540	0.2	20	300	540	1140	1260	–	–	0.25	–
		Amp/ ComboStereos	1	50	2	540	0.5	20	720	900	1020	1260	–	–	0.25	–
MIH	61	Lights Outdoor	2	25	2	840	0.2	10	1020	1440	0	420	–	–	0.35	–
		Lights Indoor	4	20	2	660	0.15	10	240	480	1080	1440	–	–	0.25	–
		Phone Charger	2	10	2	480	0.2	10	300	420	1080	1320	–	–	0.3	–
		Radio	1	10	2	540	0.2	10	300	420	1140	1260	–	–	0.25	–
		Amp/ ComboStereos	0	150	2	540	0.5	20	300	900	960	1260	–	–	0.25	–
		DVD	1	30	3	540	0.1	20	660	840	960	1050	1200	1440	0.35	–
		TV	1	150	3	240	0.1	5	300	420	720	720	1080	1440	0.35	–
		Fan	1	70	2	240	0.2	15	10	16	1170	1440	–	–	0.35	–
		Fridge/Frezer	0	300	1	1440	0.1	30	0	1440	0	0	–	–	–	–
HIH	17	Lights N	2	25	2	840	0.2	10	1020	1440	0	420	–	–	0.35	–
		Lights L	4	20	2	660	0.15	10	240	480	1080	1440	–	–	0.25	–
		Phone Charger	2	5	2	360	0.2	10	300	420	1080	1320	–	–	0.3	–
		Radio	1	10	2	540	0.2	10	300	420	1140	1260	–	–	0.25	–
		Amp/ ComboStereos	1	150	2	540	0.5	20	300	900	960	1260	–	–	0.25	–
		DVD	0	30	3	540	0.1	20	660	840	960	1080	1200	1440	0.35	–
		TV	1	150	3	240	0.2	10	300	420	720	840	1080	1440	0.35	–
		Fan	1	75	2	480	0.2	15	720	900	1170	1440	–	–	0.35	–
		Laptop/PC	0	100	2	240	0.2	10	960	1020	–	20	–	–	0.35	–
		Printer	0	90	2	60	0.2	10	–	510	750	900	–	–	0.35	–
		Electric Iron	1	1500	2	30	0.1	5	360	420	1080	1140	–	–	0.2	–
		Fridge	1	180	1	1440	0.1	30	0	1440	0	0	–	–	–	–
		Freezer	0	200	1	1440	0	30			–					
		Oven/microwave	0	2000	2	90	0.1	20	720	840	1140	1320	30	0	1440	–
		Electric kettle	0	1200	3	30	0.1	5	300	600	720	840	1140	1320		–
		Air con	0	1500	2	300	0.2	15	720	900	1020	1260	–	–	0.35	–

Legend: LIH-Households (low-Income), MIH-Households (Middle-income), HIH-Households (High-Income).

B: Public/social service.

$User_{ij}$	N_j	$Appliance_{ij}$	n_{ij}	$P_{i\,j}$ [W]	Fw_{ij} [1,2,n]	Ft_{ij} [min]	Rft_{ij} [%]	Fc_{ij} [min]	StartW1 [min]	EndW1 [min]	StartW2 [min]	EndW2 [min]	StartW3 [min]	EndW3 [min]	$Rfw_{i\,j}$[%]	Year Min
Health Centre-H	5	Lights N	8	25	2	780	0	780	0	360	1050	1440	–	–	0	–
		Lights L	18	20	2	690	0.2	480	360	1320	0	0	–	–	0.35	–
		Lights L tube	7	30	1	690	0.2	480	360	1320	0	0	–	–	0.35	–
		Phone Charger	6	10	2	360	0.2	60	0	1440	0	0	–	–	0.35	–
		Fridge	2	300	1	1440	0	30	580	1200	0	419	1201	1440		–
		Freezer	1	300	1	1440	0	30	580	1200	0	419	1201	1440		–
		Electric kettle	1	1200	3	240	0.1	5	480	540	720	780	1020	1050	0.35	–
		Fan	4	80	2	420	0.1	15	480	600	780	960	–	–	0.35	–
		Sterilizer	2	120	2	120	0.2	60	480	1020	0	0	–	–	0.35	–
		PC	1	100	2	240	0.1	30	480	600	900	1080	–	–	0.35	–
		Incubator	2	360	2	1440	0.3	720	0	1440	0	0	–	–	0	–
Water Supply System	3	Water pump	1	1000	3	120	0.2	15	360	600	720	840	1140	1320	0.35	–
School_S	1	Lights N	8	25	2	780	0	780	0	420	1050	1440	–	–	0.35	–
		Lights L	14	20	2	360	0.2	120	420	760	840	1020	–	–	0.35	–
		Lights L-tube	14	30	2	360	0.2	120	360	600	840	1020	–	–	0.2-	–
		Phone Charger	5	10	2	300	0.2	60	480	750	810	1080	–	–	0.35	–
		Cobo/radio	2	150	1	90	0.2	60	510	750	810	1080	–	–	0.35	–
		PC	1	100	2	210	0.1	120	480	720	810	1080	–	–	0.35	–
		TV	1	60	2	120	0.1	5	510	750	810	1080	–	–	0.35	–
		Fridge	1	200	2	120	0.1	5	580	1200	0	0	1201	1440	–	–
School_P	4	Lights N	2	25	2	780	0	780	0	420	1050	1440	–	–	0.35	–
		Lights L	6	20	2	360	0.2	120	420	760	840	1440	–	–	0.35	–
		Phone Charger	3	10	2	300	0.2	60	480	750	810	010	–	–	0.35	–
		Radio	2	10	1	90	0.2	60	420	480	0	0	–	–	0.35	–
Mosque/Church	2	Lights N	4	25	1	780	0	780	0	420	1050	1440	–	–	0.35	–
		Lights L	10	25	1	210	0.2	120	420	540	1020	1260	–	–	0.1	–

(*continued on next page*)

Table E.2 (*continued*)

B: Public/social service.

$User_{ij}$	N_j	$Appliance_{ij}$	n_{ij}	$P_{i\,j}$ [W]	Fw_{ij} [1,2,n]	Ft_{ij} [min]	Rft_{ij} [%]	Fc_{ij} [min]	StartW1 [min]	EndW1 [min]	StartW2 [min]	EndW2 [min]	StartW3 [min]	EndW3 [min]	$Rfw_{i\,j}$[%]	Year Min
		Sound System	1	100	1	240	0.2	90	1200	1350	0	0	–	–	0.1	–
		Phone Charger	32	10	2	300	0.2	60	480	750	810	1080	–	–	0.35	–
		Fan	4	80	2	420	0.1	15	480	600	780	960	–	–	0.35	–
Meeting Hall/ cinema	1	Lights N	3	25	2	780	0	780	0	420	1050	1440	–	–	0	–
		Lights L	8	20	2	210	0.2	120	420	540	1020	1260	–	–	0.1	–
		Ampl/Stero	2	200	2	90	0.2	60	420	840	0	0	–	–	0.35	–
		TV/ DataShow	1	150	2	120	0.1	10	540	750	810	1080	–	–	0.35	–
		Phone Charger	2	10	2	300	0.2	60	480	750	810	1080	–	–	0.35	–
		Fan	4	80	2	300	0.1	15	420	540	1020	1260	–	–	0.35	2
Police Station	1	Lights N	2	25	2	780	0	780	0	360	1050	1440	–	–	0	–
		Lights L	4	20	2	690	0.2	480	420	1320	0	0	–	–	0.35	–
		Phone Charger	2	10	2	360	0.2	60	0	1440	0	0	–	–	0.35	–
		Radio	1	10	2	180	0.2	60	420	1020	0	0	–	–	0.35	–
		Fridge	1	200	1	1440	0	30	580	1200	0	509	1201	1440	–	5
		PC	1	100	2	210	0.1	120	480	720	810	1080	–	–	0.35	3
		TV	1	150	2	120	0.1	10	510	750	810	1080	–	–	0.35	3
		Printer	1	90	3	540	0.1	60	510	750	900	1080	- 1200	1440	0.35	3
		Fan	2	80	2	420	0.1	15	420	540	1020	1260	–	–	0.35	2
Secretary of the locality	1	Lights N	2	25	2	780	0	780	0	360	1050	01440	–	–	0	–
		Lights L	6	20	2	690	0.2	60	420	1320	0	0	–	–	0.35	–
		TV	1	150	2	120	0.1	10	510	750	810	960	–	–		5
		Phone Charger	4	10	2	360	0.2	60	480	600	810	900	–	–	0.35	–
		PC	1	100	3	210	0.1	120	510	750	900	1050	1200	1440	0.25	5
		Printer	1	100	3	540	0.1	60	510	750	900	1050	1200	1440	–	6
		Radio	1	10	2	420	0.2	60	420	720	810	900	–	–	0.35	–
		Fan	2	80	2	420	0.1	30	420	540	1020	1260	–	–	0.35	2
		Fridge	1	200	1	1440	0	30	580	1200	0	509	1201	1440		–
Street lights	266	Streetlights	164	400	2	780	0	780	0	360	1050	1440	–	–	0	–
			50	70	2	780	0	780	0	360	1050	1440	–	–	0	–
			52	70	2	780	0	780	0	360	1050	1440	–	–	0	–
			16	400	2	780	0	780	0	360	1050	1440	–	–	0	4
FUNAE Offices	3	Lights N	3	25	2	780	0	780	0	360	1050	1440	–	–	0	–
		Lights L	2	30	2	540	0.2	480	360	1320	0	0	–	–	0.35	–
		Lights L	3	20	2	690	0.2	480	420	1320	0	0	–	–	0.35	–
		TV	1	150	2	120	0.1	5	510	750	810	1000	–	–	0.35	–
		Phone Charger	2	10	2	360	0.2	60	0	1440	0	0	–	–	0.35	–
		PC	1	100	3	540	0.1	60	510	750	900	1080	1200	1440	0.35	–
		Radio	1	10	2	180	0.2	120	420	1020	0	0	–	–	0.35	–
		Printer	1	90	3	540	0.1	60	510	720	900	1080	1200	1440	0.35	–
		Fridge	1	400	1	1440	0	30	580	1200	0	509	1201	1440		–
		Air Con	1	1500	2	420	0.2	150	540	900	1020	1260	–	–	0.35	–
		Kettle	1	1200	3	420	0.1	5	480	540	720	780	1020	1080	0.1	4

C: Productive/commercial services

$User_{ij}$	N_j	$Appliance_{ij}$	n_{ij}	$P_{i\,j}$ [W]	Fw_{ij} [1,2,n]	Ft_{ij} [min]	Rft_{ij} [%]	Fc_{ij} [min]	StartW1 [min]	EndW1 [min]	StartW2 [min]	EndW2 [min]	StartW3 [min]	EndW3 [min]	$Rfw_{i\,j}$[%]	Year Min
Metalwork	10	Lights N	1	25	2	780	0	780	0	420	1020	1440	–	–	0	–
		Lights L	2	20	2	360	0.2	120	420	600	840	1020	–	–	0.35	–
		Phone Charger	1	10	2	240	0.2	60	540	750	850	960	–	–	0.35	–
		Welding machine	1	3300	2	300	0.5	10	420	750	840	1050	–	–	0.1	–
		Annglehgrinder	1	1900	2	360	0.5	10	420	750	840	1050	–	–	0.1	–
Carpentry	7	Lights N	1	25	2	780	0	780	0	420	1050	1440	–	–	0	–
		Lights L	1	20	2	360	0.2	30	420	600	840	1020	–	–	0.1	–
		Electric chainsaw	1	700	2	360	0.2	30	480	720	840	1080	–	–	0.1	4
Small grocery shops	6	Lights N	1	25	2	780	0	780	0	420	1050	1440	–	–	0	–
		Lights L	2	20	2	780	0.2	10	60	480	1020	1320	–	–	0.1	–
		Radio/ ComboSterios	1	60	2	540	0.5	20	480	780	1140	1260	–	–	0.25	–
		DVD	1	30	3	540	0.1	20	660	840	960	1080	1200	1440	0.35	–
		TV	1	150	3	240	0.1	5	300	420	720	840	1080	1440	0.35	–
		Freezer	1	200	1	1440	0	30	0	1440	0	0	–	–	0	3
		Fridge	1	250	1	1440	0.1	30	0	1440	0	03	–	–	0	–
		Phone charger	2	7	2	300	0.2	60	60	480	1020	1320	–	–	0.1	–
		PC	1	100	2	360	0.1	10	540	720	900	1140	–	–	0.35	–

(*continued on next page*)

Table E.2 (*continued*)

C: Productive/commercial services															
$User_{ij}$	N_j	$Appliance_{ij}$	n_{ij}	$P_{i\ j}$ [W]	Fw_{ij} [1,2,n]	Ft_{ij} [min]	Rft_{ij} [%]	Fc_{ij} [min]	StartW1 [min]	EndW1 [min]	StartW2 [min]	EndW2 [min]	StartW3 [min]	EndW3 [min]	$Rfw_{i\ j}$[%]	Year Min
		Printer	1	100	3	180	0.1	10	510	750	900	1140	–	–	0.35	–
		Electric kettle	1	1500	3	420	0.1	5	480	540	720	780	1020	1080	0.1	–
		Fan	1	75	2	300	0.2	15	720	900	1020	1260	–	–	0.35	–
Bars/Ristorants	10	Lights N	1	25	2	780	0	780	0	420	1050	1440	–	–	0	–
		Lights L	2	20	2	240	0.1	240	420	540	900	1080	–	–	0.1	–
		Radio/ ComboSterios	1	100	2	720	0.2	240	480	780	960	1080	–	–	0.2	–
		DVD	1	30	3	540	0.1	20	660	840	960	1080	1200	1440	0.35	–
		TV	1	150	3	240	0.1	5	300	420	720	840	1080	1440	0.35	–
		Fridge	1	250	1	1440	0.1	30	360	660	1320	1440	0	360	0	–
		Phone charger	2	7	2	300	0.2	60	60	480	1020	1320			0.1	–
		PC	1	100	3	540	0.1	60	510	750	900	1080	1200	1440	0.35	–
		Fan	1	75	2	300	0.2	15	720	900	1020	1260			0.35	–
		Electric kettle	1	1500	3	420	0.1	5	480	540	720	780	1020	1080	0.1	–
Tents	6	Lights L/Indoor	1	20	2	720	0.2	30	360	480	1080	1260	–	–	0.3	–
		Radio	1	7	1	100	0.1	10	420	1080	0	0	–	–	0.35	–
		Charger	2	10	2	300	0.2	60	540	750	850	960	–	–	0.35	–
Barbershop	2	Lights N	1	25	2	780	0	780	0	420	1050	1440	–	–	0	–
		Lights L	2	20	2	240	0.1	240	420	540	900	1080	–	–	0.1	–
		Cutting/Clippet Machine	2	40	2	0.1	240	20	540	660	840	960	–	–	0.1	–
		Hair dryer	2	1000	2	0.1	240	20	540	660	840	960	–	–	0.1	–
		Phone Charger	2	10	2	300	0.2	60	540	750	850	960	–	–	0.35	–
		TV	1	150	3	240	0.1	5	300	420	720	840	1080	1440	0.35	–
		Radio/ ComboSterios	1	60	2	720	0.2	240	480	780	960	1080	–	–	0.2	–
		DVD	1	30	3	540	0.1	20	660	840	960	1080	1200	1440	0.35	–
Mobile Tower Anthena	3	Mobile System	1	5000	1	1440	0	60	0	1440	–	–	–	–	0.5	–

Table E.3
Input details on adopted assumptions for evolving demands for SCN1 (A) and SCN2 (B). The Adopted/owned appliances include Baseline SCN0.

A: SCN1- (2%Growth)				
Type of appliances/user	Low-income households	Middle-income households	High-income households	Public services	Commercial activities
	Appliance () Year-%share	Appliance () Year-% share	Appliance () Year-%share	Appliance () Year-%share (user/class)	Appliance () Year-% share (user/class)
Outdoor lights (1), indoor lights (2), phone charger (3) Radio (4), stereo (5), TV (7), Laptop/Pc(8), Printer (9)	(5) Y2–5%; (7) Y5–10%	(5)(7)(8) Y1,Y2, Y3–10%;	(7)(8) Y3, Y5–10%;	(7) Y3–10% (FO;PO; HAP) (8) Y3–5%(PO;HAP); (9) Y3-(PO;HAP)	Baseline
Fan (10), air conditioner (11) electric iron (12), Fridge/freezer(13), Oven/microwave (15), electric kettle(16)	(10) Y2–10%	(10) Y3–10%; (11) (12)(13)(16) Y3–5%;	(11) Y5–10%; (15) Y3–5%;	(10) Y1–5% (Mhall; HAP); (10) Y3 (PO); (13) Y3–5% (Mhall), (13) Y5 (PO); (16) Y1–10% (FO,)	Baseline
Medical equipment (17), Public light (18), Metalwork (19)	–	–	–	(18) Y1–100%)	Baseline
Water pump(24), Grind mill(25), carpentry (26), Fuel station (27), Tailor machine (28)	–	–	–	(24) Y5–5% (CM;Pschool;Sschool)	(25)Y4 (26) Y3; (28) Y3

B: SCN2- (2.8%Growth)					
Type of appliances owned/user	Low-income households	Middle-income households	High-income households	Public services	Commercial activities
	Appliance () Year-% share	Appliance () Year-% share	Appliance () Year-%share	Appliance () Year-%share (user/class)	Appliance () Year-% share (user/class)
Outdoor lights (1), indoor lights (2), phone charger (3) Radio (4), stereo (5), TV (7), Laptop/Pc(8), Printer (9)	(5) Y1–5%; (7) Y5–20%	(5)(7)(8) Y1,Y2, Y3–10%;	SCN1+	SCN1 + (7) Y3–10%(FO; PO;HAP/); (8) Y3–5%(PO;HAP); (9) Y3-(PO;HAP)	–
Fan (10), air conditioner (11) electric iron (12), Fridge/freezer(13), Oven/ microwave(15), electric kettle(16)	(10) Y1–20%; (12) Y2–10%; (16) Y3–5%	(10) Y3–10%; (11) (12)(13)16) Y3–10%;		(10) Y1–5% (Mhall;HAP;); (10)-Y3 (PO); (13) Y3–5%(Mhall), (13) Y5 (PO); (16) Y1–10%(FO,)	–
Medical equipment (17), Public light (18), Weldering/solder (19)				(18)-(Y1–100%);	–
Water pump (24), Grind mill(25), carpentry (26), Fuel station (27), Tailor machine (28)				(24) Y5–5%(CM;Pschool;Sschool)	SCN1 (27)Y3

Y = year.

Appendix F. Rural electrification planning methodologies

The tools, OnSSET and iNTIGIS for instance, were previously chosen among others as applicable and/or adaptable for this study and HOMER for result comparisons. Nevertheless, the adopted tool, GISELE_v01 (GIS for electrification) is also a fully open-source tool written in Python (Corigliano et al., 2020). Despite having some limitations (demand assessment, technology options), its modelling features best fit our study modelling requirements as per our previous review insights (Silinto et al., 2025) which is concerned to rural electrification planning's comprehensiveness and multidimensions[10]: ease of customizability and applicability, geospatial modelling approaches and advanced algorithms for clustering analysis and grid/network design, sizing and techno-economic optimization of hybrid microgrids, applied for the context of rural Mozambique. Differently to the aforementioned GIS-based tools, GISELE evaluates technology options in a high-level granularity, to identify the least-cost off- and on-grid electrification solutions in both small- and large-scale applications.

Appendix Table G1
Summary of modelling capabilities.

Model/ method	User-friendliness/ level[c]	Energy modelling (designs/sizing) (A)	Geospatial planning (B)	Network design (C)	Analysis	References
HOMER[a]	Yes (high)	Yes	No	No	single-objective function for minimizing NPC	(HOMER, 2019)
iHOGA[a]	Yes (medium)	Yes	No	No	Min NPC using genetic algorithms	(Saiprasad et al., 2018)
InTIGIS[a]	Yes (high)	Yes	Yes	(Yes)	levelized electricity cost (LEC)	(Domínguez & Pinedo-Pascua, 2009)
GEOSIM[(a)]	Yes (medium)	Yes	yes	yes	commercial softwares	
ONSSET[b]	Yes(medium)	Yes	yes	(yes)	LCOEs -Size mono-energy source micro-grids -simple energy balance to meet an average peak demand in every settlement; -Electric grid topology simplified and terrain morphology not considered	(Mentis et al., 2015) (Korkovelos et al., 2019)
GISEle[b]	Yes(High)	Yes	Yes	Yes	LCOE: addresses the problem of electrification considering, all electric grid topology including terrain morphology and its costs, - considers hybrid (solar+wind+hydro) microgrids & costs	(Corigliano et al., 2020) (Vinicius et al., 2021)

[a] Commercial software.
[a] Free software but depends on a commercial software ArcGiS and of an old/outdated windows 7 which limits its functionalities.
[b] Free open-source tools.
[c] (Silinto, van der Laag Yamu, Zuidema, & Faaij, 2025).

References

ADB. (2017). *Deployment of hybrid renewable energy systems in minigrids*.

Allington, L., Cannone, C., Pappis, I., Cervantes Barron, K., Usher, W., Pye, S., Howells, M., Taliotis, C., Sundin, C., Sridharan, V., Ramos, E., Brinkerink, M., Deane, P., Gritsevskyi, A., Moura, G., Rouget, A., Wogan, D., Barcelona, E., & Rogner, H. (2023). *CCG Starter Data Kit: Mozambique (v2.0)*. In *Zenodo*. https://doi.org/10.5281/zenodo.7539477.

Angel, J. P. B., Dominguez, J., Guerra, J. A., Arribas, L., & Pinedo, I. (2011). *Characterization of hybrid systems for rural electrification with renewable energies using geographic information systems (Issue June 2014). 1135–9420*.

Arias, A. P. (2015). *IntiGIS 2. 0 : Objetivos y propuesta metodológica. Análisis de competitividad tecnológica en Ghana*. Universidad Complutense de Madrid.

Arnold, J. G., Srinivasan, R., Muttiah, R. S., & Williams, J. R. (1998). Large area hydrologic modeling and assessment part I: Model development. *Journal of the American Water Resources Association, 34*(1), 73–89. https://doi.org/10.1111/j.1752-1688.1998.tb05961.x

Bhatia, M., & Angelou, N. 2015. Beyond connections: Energy access redefined (ESMAP Technical Report 008/15).

Beck, H. E., de Roo, A., & van Dijk. (2015). Global Maps of Streamflow Characteristics Based on Observations from Several Thousand Catchments*. *Journal of Hydrometeorology, 16*(4), 1478–1501. https://doi.org/10.1175/JHM-D-14-0155.1

Bhattacharyya, S. C. (2012). Review of alternative methodologies for analysing off-grid electricity supply. *Renewable and Sustainable Energy Reviews, 16*(1), 677–694. https://doi.org/10.1016/j.rser.2011.08.033

Boithias, L., Sauvage, S., Lenica, A., Roux, H., Abbaspour, K. C., Larnier, K., … Sánchez-Pérez, J. M. (2017). Simulating flash floods at hourly time-step using the SWAT model. *Water (Switzerland), 9*(12), 1–25. https://doi.org/10.3390/w9120929

Cader, C., Pelz, S., Radu, A., & Blechinger, P. (2018). Overcoming data scarcity for energy access planning with open data - the example of Tanzania. *The International Archives of the Photogrammetry, Remote Sensing and Spatial Information Sciences, XLII-4/W8(4W8)*, 23–26. https://doi.org/10.5194/isprs-archives-XLII-4-W8-23-2018

CIESIN. (2020). *High Resolution Settlement Layer. Center for International Earth Science Information Network*. Earth Institute Columbia University. https://ciesin.columbia.edu/data/hrsl/.

Cole, W., & Frazier, A. W. (2023). *Cost Projections for Utility-Scale Battery Storage: 2023 Update. National Renewable Energy Laboratory, June, 20*.

Come Zebra, E. I., van der Windt, H. J., Nhumaio, G., & Faaij, A. P. C. (2021). A review of hybrid renewable energy systems in mini-grids for off-grid electrification in developing countries. *Renewable and Sustainable Energy Reviews, 144*(July 2020). https://doi.org/10.1016/j.rser.2021.111036

Corigliano, S., Carnovali, T., Edeme, D., & Merlo, M. (2020). Holistic geospatial data-based procedure for electric network design and least-cost energy strategy. *Energy for Sustainable Development, 58*, 1–15. https://doi.org/10.1016/j.esd.2020.06.008

Dile, Y., Srinivasan, R., & George, C. (2022). *QGIS interface for SWAT+: QSWAT+: Vol. 2.2 (issue March, p. 118)*.

Domínguez, J., & Pinedo-Pascua, I. (2009). GIS Tool for Rural Electrification with Renewable Energies in Latin America. In *2009 International Conference on Advanced Geographic Information Systems & Web Services* (pp. 171–176). https://doi.org/10.1109/GEOWS.2009.25

Dufo-López, R., Cristóbal-Monreal, I. R., & Yusta, J. M. (2016). Optimisation of PV-wind-diesel-battery stand-alone systems to minimise cost and maximise human development index and job creation. *Renewable Energy, 94*, 280–293. https://doi.org/10.1016/j.renene.2016.03.065

E4Growing. (2022). GISELE. Http://Www.E4g.Polimi.It/?Page_id=524. https://github.com/Energy4Growing/gisele_v01.

Elia, A., Kamidelivand, M., Rogan, F., Gallachóir, Ó., & B.. (2021). Impacts of innovation on renewable energy technology cost reductions. *Renewable and Sustainable Energy Reviews, 138*(September 2020), Article 110488. https://doi.org/10.1016/j.rser.2020.110488

ESMAP. (2022). Mini grids for half a billion people. In Mini Grids for Half a Billion People. World Bank. https://doi.org/10.1596/38082.

ESRI. (2021). Esri land cover. https://livingatlas.arcgis.com/landcover/.

[10] Delivers context-specific solutions on: techno-economical dimension, socio-economic and demand focused development indicators, geographic dimension related to the assessment of local resources and territory peculiarities, environmental impact and regulatory framework.

Etherington, T. R. (2016). Least-cost Modelling and Landscape Ecology: Concepts, applications, and Opportunities. *Current Landscape Ecology Reports, 1*(1), 40–53. https://doi.org/10.1007/s40823-016-0006-9

Falchetta, G., Pachauri, S., Byers, E., Danylo, O., & Parkinson, S. C. (2020). Satellite Observations Reveal Inequalities in the Progress and Effectiveness of recent Electrification in Sub-Saharan Africa. *One Earth, 2*(4), 364–379. https://doi.org/10.1016/j.oneear.2020.03.007

Falchetta, G., Pachauri, S., Parkinson, S., & Byers, E. (2019). A high-resolution gridded dataset to assess electrification in sub-Saharan Africa. *Scientific Data, 6*(1), 1–9. https://doi.org/10.1038/s41597-019-0122-6

GADM. (2022). GADM maps and data: Global administrative boundaries. Web site. https://geodata.ucdavis.edu/gadm/gadm4.1/shp/gadm41_MOZ_shp.zip.

Glenk, G., Meier, R., & Reichelstein, S. (2021). Cost Dynamics of Clean Energy Technologies. *Schmalenbach Journal of Business Research, 73*(2), 179–206. https://doi.org/10.1007/s41471-021-00114-8

GRDC (Global Runoff Data Centre). (2021). The GRDC - The world-wide repository of river discharge data and associated metadata. https://www.bafg.de/GRDC/EN/01_GRDC/grdc_node.html.

Hasan, M. M., & Wyseure, G. (2018). Impact of climate change on hydropower generation in Rio Jubones Basin, Ecuador. *Water Science and Engineering, 11*(2), 157–166. https://doi.org/10.1016/j.wse.2018.07.002

Herraiz-Cañete, Á., Ribó-Pérez, D., Bastida-Molina, P., & Gómez-Navarro, T. (2022). Forecasting energy demand in isolated rural communities: A comparison between deterministic and stochastic approaches. *Energy for Sustainable Development, 66*, 101–116. https://doi.org/10.1016/j.esd.2021.11.007

HOMER. (2019). *HOMER Energy Bibliography*. Retrieved 1 November 2019, from Homer Energy https://microgridnews.com/homer-energy-bibliography/.

IEA. (2020). *Renewables 2020 - Analysis and forecast to 2025. In Plastics Engineering (Vol. 74, Issue 9)*.

IEA, IRENA, UNSD, Bank, W, & WHO. (2020). *Tracking SDG7: The Energy Progress Report, 2020*.

IEA, IRENA, UNSD, World_Bank, & WHO. (2023). *Tracking SDG7: The Energy Progress Report*.

IEA-ETSAP, & IRENA. (2015). *Hydropower|Technology brief*.

IED. (2021). GEOSIM - IED-Software-Catalogue. Retrieved January 12, 2021, from https://www.ied-sa.fr/images/Logiciels/en/IED-Software-Catalogue.pdf.

Ikejemba, E. C. X., Mpuan, P. B., Schuur, P. C., & Van Hillegersberg, J. (2017). The empirical reality & sustainable management failures of renewable energy projects in Sub-Saharan Africa (part 1 of 2). *Renewable Energy, 102*, 234–240. https://doi.org/10.1016/j.renene.2016.10.037

Ikejemba, E. C. X., Schuur, P. C., Van Hillegersberg, J., & Mpuan, P. B. (2017). Failures & generic recommendations towards the sustainable management of renewable energy projects in Sub-Saharan Africa (part 2 of 2). *Renewable Energy, 113*, 639–647. https://doi.org/10.1016/j.renene.2017.06.002

INE. (2017). *IV RGPH 2017*, 10-22:38-25. InINE http://www.ine.gov.mz/operacoes-estatisticas/censos/censo-2007/censo-2017.

IRENA. (2016). *Innovation outlook mini-grids*.

IRENA. (2022). IRENA (2022), Renewable Power Generation costs in 2021, International Renewable Energy Agency, Abu Dhabi. ISBN 978–92–9260-452-3. In International Renewable Energy Agency.

Jarvis, A., Guevara, E., Reuter, H. I., & Nelson, A. D. (2008). *Hole-filled SRTM for the globe : version 4 : data grid.* Web Publication/Site, CGIAR Consortium for Spatial Information. http://srtm.csi.cgiar.org.

IRENA. (2024). Renewable power generation costs in 2023. In *International Renewable Energy Agency*. Abu Dhabi.

Kemausuor, F., Adkins, E., Adu-Poku, I., Brew-Hammond, A., & Modi, V. (2014). Electrification planning using network planner tool: The case of Ghana. *Energy for Sustainable Development, 19*(1), 92–101. https://doi.org/10.1016/j.esd.2013.12.009

Korkovelos, A., Khavari, B., Sahlberg, A., Howells, M., & Arderne, C. (2019). The role of open access data in geospatial electrification planning and the achievement of SDG7. An onsset-based case study for Malawi. *Energies, 12*(7). https://doi.org/10.3390/en12071395

Lehner, B., Verdin, K., & Jarvis, A. (2008). New Global Hydrography Derived from Spaceborne Elevation Data. *Eos, Transactions American Geophysical Union, 89*(10), 93. https://doi.org/10.1029/2008EO100001

Lian, J., Zhang, Y., Ma, C., Yang, Y., & Chaima, E. (2019). A review on recent sizing methodologies of hybrid renewable energy systems. *Energy Conversion and Management, 199*(September), Article 112027. https://doi.org/10.1016/j.enconman.2019.112027

Lloyd, C. T. (2017). High resolution global gridded data for use in population studies. *ISPRS - International Archives of the Photogrammetry, Remote Sensing and Spatial Information Sciences, XLII-4/W2*(4W2), 117–120. https://doi.org/10.5194/isprs-archives-XLII-4-W2-117-2017

Lombardi, F., Balderrama, S., Quoilin, S., & Colombo, E. (2019). Generating high-resolution multi-energy load profiles for remote areas with an open-source stochastic model. *Energy, 177*, 433–444. https://doi.org/10.1016/j.energy.2019.04.097

Lorenzoni, L., Cherubini, P., Fioriti, D., Poli, D., Micangeli, A., & Giglioli, R. (2020). Classification and modeling of load profiles of isolated mini-grids in developing countries: A data-driven approach. *Energy for Sustainable Development, 59*, 208–225. https://doi.org/10.1016/j.esd.2020.10.001

Lucas, P. L., Dagnachew, A. G., & Hof, A. F. (2017). *Towards universal electricity access in sub-Saharan Africa: A quantitative analysis of technology and investment requirements*.

Mentis, D., Welsch, M., Fuso Nerini, F., Broad, O., Howells, M., Bazilian, M., & Rogner, H. (2015). A GIS-based approach for electrification planning-A case study on Nigeria. *Energy for Sustainable Development, 29*, 142–150. https://doi.org/10.1016/j.esd.2015.09.007

MIREME. (2018). *Integrated master plan: Mozambique power system development final report*.

Moiz, A., Kawasaki, A., Koike, T., & Shrestha, M. (2018). A systematic decision support tool for robust hydropower site selection in poorly gauged basins. *Applied Energy, 224*(March), 309–321. https://doi.org/10.1016/j.apenergy.2018.04.070

Moner-Girona, M., Puig, D., Mulugetta, Y., Kougias, I., AbdulRahman, J., & Szabó, S. (2018). Next generation interactive tool as a backbone for universal access to electricity. *WIREs Energy and Environment, 7*(6), Article e305. https://doi.org/10.1002/wene.305

Monteiro, C., Ramirez-Rosado, I. J., Miranda, V., Zorzano-Santamaria, P. J., Garcia-Garrido, E., & Fernandez-Jimenez, L. A. (2005). GIS Spatial Analysis Applied to Electric Line Routing Optimization. *IEEE Transactions on Power Delivery, 20*(2), 934–942. https://doi.org/10.1109/TPWRD.2004.839724

Neitsch, S. L., Arnold, J. G., Kiniry, J. R., & Williams, J. R. Soil & water assessment tool theoretical documentation version 2009. 2011. Texas Water Resources Institute, 1-647. https://doi.org/10.1016/j.scitotenv.2015.11.063.

Nkhoma, L., Ngongondo, C., Dulanya, Z., & Monjerezi, M. (2021). Evaluation of integrated impacts of climate and land use change on the river flow regime in wamkurumadzi river, shire basin in Malawi. *Journal of Water and Climate Change, 12*(5), 1674–1693. https://doi.org/10.2166/wcc.2020.138

NP. (2019). *Network Planner*. Columbia University. https://qsel.columbia.edu/network-planner/.

ONSSET. (2021). Open source spatial electrification tool - Publications. http://www.onsset.org/publications.html.

Peters, J., Sievert, M., & Toman, M. A. (2019). Rural electrification through mini-grids: Challenges ahead. *Energy Policy, 132*(May), 27–31. https://doi.org/10.1016/j.enpol.2019.05.016

Petrelli, M., Fioriti, D., Berizzi, A., & Poli, D. (2021). Multi-Year Planning of a Rural Microgrid considering Storage Degradation. *IEEE Transactions on Power Systems, 36*(2), 1459–1469. https://doi.org/10.1109/TPWRS.2020.3020219

Pfenninger, S., DeCarolis, J., Hirth, L., Quoilin, S., & Staffell, I. (2017). The importance of open data and software: Is energy research lagging behind? *Energy Policy, 101*(July 2016), 211–215. https://doi.org/10.1016/j.enpol.2016.11.046

Pfenninger, S., Hawkes, A., & Keirstead, J. (2014). Energy systems modeling for twenty-first century energy challenges. *Renewable and Sustainable Energy Reviews, 33*, 74–86. https://doi.org/10.1016/j.rser.2014.02.003

Pfenninger, S., Hirth, L., Schlecht, I., Schmid, E., Wiese, F., Brown, T., … Wingenbach, C. (2018). Opening the black box of energy modelling: Strategies and lessons learned. *Energy Strategy Reviews, 19*, 63–71. https://doi.org/10.1016/j.esr.2017.12.002

Pfenninger, S., & Staffell, I. (2016). Long-term patterns of European PV output using 30 years of validated hourly reanalysis and satellite data. *Energy, 114*, 1251–1265. https://doi.org/10.1016/j.energy.2016.08.060

Prina, M. G., Manzolini, G., Moser, D., Nastasi, B., & Sparber, W. (2020). Classification and challenges of bottom-up energy system models - a review. *Renewable and Sustainable Energy Reviews, 129*, Article 109917. https://doi.org/10.1016/j.rser.2020.109917

Riva, F., Ahlborg, H., Hartvigsson, E., Pachauri, S., & Colombo, E. (2018). Electricity access and rural development: Review of complex socio-economic dynamics and causal diagrams for more appropriate energy modelling. *Energy for Sustainable Development, 43*, 203–223. https://doi.org/10.1016/j.esd.2018.02.003

Riva, F., Tognollo, A., Gardumi, F., & Colombo, E. (2018). Long-term energy planning and demand forecast in remote areas of developing countries: Classification of case studies and insights from a modelling perspective. *Energy Strategy Reviews, 20*, 71–89. https://doi.org/10.1016/j.esr.2018.02.006

Roth, V., & Lemann, T. (2016). Comparing CFSR and conventional weather data for discharge and soil loss modelling with SWAT in small catchments in the Ethiopian Highlands. *Hydrology and Earth System Sciences, 20*(2), 921–934. https://doi.org/10.5194/hess-20-921-2016

Saiprasad, N., Kalam, A., & Zayegh, A. (2018). Comparative study of optimization of HRES using HOMER and iHOGA software. *Journal of Scientific & Industrial Research, 77*(12), 677–683.

Silinto, B. F., Ededme, D., Corigliano, S., Dimovskic, A., Merlo, M., Zuidema, C., & Faaij, A. (2025). An integrated geospatial modelling framework of hybrid microgrid sizing for rural electrifica on planning. 1-27.

Schubert, E., Sander, J., Ester, M., Kriegel, H. P., & Xu, X. (2017). DBSCAN revisited, revisited: Why and how you should (still) use DBSCAN. *ACM Transactions on Database Systems, 42*(3). https://doi.org/10.1145/3068335

Silinto, B. F., van der Laag Yamu, C., Zuidema, C., & Faaij, A. P. C. (2025). Hybrid renewable energy systems for rural electrification in developing countries: A review on energy system models and spatial explicit modelling tools. *Renewable and Sustainable Energy Reviews, 207*(March 2021), 114916. https://doi.org/10.1016/j.rser.2024.114916

Staffell, I., & Pfenninger, S. (2016). Using bias-corrected reanalysis to simulate current and future wind power output. *Energy, 114*, 1224–1239. https://doi.org/10.1016/j.energy.2016.08.068

Stevanato, N., Lombardi, F., Guidicini, G., Rinaldi, L., Balderrama, S. L., Pavičević, M., … Colombo, E. (2020). Long-term sizing of rural microgrids: Accounting for load evolution through multi-step investment plan and stochastic optimization. *Energy for Sustainable Development, 58*, 16–29. https://doi.org/10.1016/j.esd.2020.07.002

Tatem, A. J. (2017). WorldPop, open data for spatial demography. *Scientific Data, 4*(1), Article 170004. https://doi.org/10.1038/sdata.2017.4

Theo, W. L., Lim, J. S., Ho, W. S., Hashim, H., & Lee, C. T. (2017). Review of distributed generation (DG) system planning and optimisation techniques: Comparison of numerical and mathematical modelling methods. *Renewable and Sustainable Energy Reviews, 67*, 531–573. https://doi.org/10.1016/j.rser.2016.09.063

UNEP-WCMC, & IUCN. (2022). *Protected Planet: The World Database on Protected areas (WDPA) and World Database on Other Effective Area-based Conservation measures (WD-OECM)* [Online],. Cambridge, UK: UNEP-WCMC and IUCN www.protectedplanet.net.

Urban, F., Benders, R. M. J., & Moll, H. C. (2007). Modelling energy systems for developing countries. *Energy Policy, 35*(6), 3473–3482. https://doi.org/10.1016/j.enpol.2006.12.025

van Beeck, N., van Groenendaal, W., van Helden, W., & Ouwens, C. D. (2000). A New Method for Local Energy Planning in developing Countries. World Renewable Energy Congress VI, 2465–2468.https://doi.org/10.1016/b978-008043865-8/50538-9.

Vinicius, G. T. F., Silvia, C., Aleksandar, D., Massimo, B., & Marco, M. (2021). Rural electrification planning based on graph theory and geospatial data: A realistic topology oriented approach. *Sustainable Energy, Grids and Networks, 28*, Article 100525. https://doi.org/10.1016/j.segan.2021.100525

Zebra, E. I. C., van der Windt, H. J., Olubayo, B., Nhumaio, G., & Faaij, A. P. C. (2023). Scaling up the electricity access and addressing best strategies for a sustainable operation of an existing solar PV mini-grid: A case study of Mavumira village in Mozambique. *Energy for Sustainable Development, 72*(August 2022), 58–82. https://doi.org/10.1016/j.esd.2022.11.012